TITLE:

Keratinocytes Drive the Epithelial Hyperplasia Key to Sea Lice Resistance in Coho Salmon

AUTHORS:

S.J. Salisbury[1*†], R. Ruiz Daniels[1†], S.J. Monaghan[2], J.E. Bron[2], P.R. Villamayor[1,3], O. Gervais[1], M.D. Fast[4], L. Sveen[5], R.D. Houston[6], N. Robinson[5,7*], and D. Robledo[1*]

ASSOCIATIONS:

1. The Roslin Institute and Royal (Dick) School of Veterinary Studies, University of Edinburgh, Edinburgh, UK.

2. Institute of Aquaculture, University of Stirling, Stirling, UK.

3. University of Santiago de Compostela, Santiago de Compostela, Spain.

4. Atlantic Veterinary College, University of Prince Edward Island, Charlottetown, Canada.

5. Nofima AS, Tromsø, Norway.

6. Benchmark Genetics, 1 Pioneer Building, Edinburgh Technopole, Milton Bridge, Penicuik, UK.

7. Sustainable Aquaculture Laboratory -Temperate and Tropical (SALTT), Deakin University, Victoria 3225, Australia.

* Corresponding authors: sarahsalisbury13@gmail.com, nicholas.robinson@nofima.no, diego.robledo@roslin.ed.ac.uk,

† Co-first authors

25 **KEYWORDS:** snRNAseq, salmon, aquaculture, disease, parasite, sea lice, cell type, skin,

26 immunity, wound-healing

ABSTRACT:

Background:

Salmonid species have followed markedly divergent evolutionary trajectories in their interactions with sea lice. While sea lice parasitism poses significant economic, environmental, and animal welfare challenges for Atlantic salmon (*Salmo salar*) aquaculture, coho salmon (*Oncorhynchus kisutch*) exhibit near-complete resistance to sea lice, achieved through a potent epithelial hyperplasia response leading to rapid louse detachment. The molecular mechanisms underlying these divergent responses to sea lice are unknown.

Results:

We characterised the cellular and molecular responses of Atlantic salmon and coho salmon to sea lice using single-nuclei RNA sequencing. Juvenile fish were exposed to copepodid sea lice (*Lepeophtheirus salmonis*), and lice-attached pelvic fin and skin samples were collected 12h, 24h, 36h, 48h, and 60h after exposure, along with control samples. Comparative analysis of control and treatment samples revealed an immune and wound-healing response that was common to both species, but attenuated in Atlantic salmon, potentially reflecting greater sea louse immunomodulation. Our results revealed unique but complementary roles of three layers of keratinocytes in the epithelial hyperplasia response leading to rapid sea lice rejection in coho salmon. Our results suggest that basal keratinocytes direct the expansion and mobility of intermediate and, especially, superficial keratinocytes, which eventually encapsulate the parasite.

Conclusion:

Our results highlight the key role of keratinocytes to coho salmon's sea lice resistance, and the diverged biological response of the two salmonid host species when interacting with this parasite. This study has identified key pathways and candidate genes that could be manipulated using various biotechnological solutions to improve Atlantic salmon sea lice resistance.

INTRODUCTION:

Parasitism by sea lice is one of the greatest economic, environmental, and animal welfare issues facing the Atlantic salmon (*Salmo salar*, Linnaeus, 1758) aquaculture industry, with annual global costs exceeding £700 million [1]. Sea lice species, including the northern hemisphere's *Lepeophtheirus salmonis* (Krøyer, 1837) and the southern hemisphere's *Caligus rogercresseyi* [2], feed on salmon skin and fins, causing chronic open wounds in Atlantic salmon that can contribute to secondary infections [3]. Additionally, sea lice significantly reduce the market value of aquaculture fish – infestations have been estimated to cost US$0.46/kg of biomass [4] – and can also cause considerable impacts on wild salmonids [5]. A variety of treatment strategies have been developed to mitigate sea lice infestations in Atlantic salmon aquaculture, but these can be costly, ineffective, environmentally-damaging, and cause reduced animal welfare [6]. For example, sea lice have evolved increasing resistance to the costly and potentially environmentally damaging chemical parasiticides that have historically been commonly applied to salmon aquaculture pens [5,7]. Preventative methods, particularly those improving the innate resistance of Atlantic salmon to sea lice, are therefore considered a more effective route to address this problem [6].

Relatively high heritabilities for sea lice resistance in Atlantic salmon [e.g., 8-10] suggest that selective breeding should be effective, particularly when informed by genotype information via genomic selection [11, 12]. However, counts of sessile lice are the only

measure of resistance that is currently used, and genetic variation in the immune response of Atlantic salmon has been difficult to assess. In addition, despite the identification of some significant QTL [*e.g.*, 13-15], sea lice resistance has proven to be a polygenic trait [11]. Given the absence of loci of large effect to target, the relatively long generation time of Atlantic salmon (3-4 years), and that modern salmon breeding programs must include multiple additional traits in their breeding goal, selective breeding is unlikely to result in clear improvements to sea lice resistance in the short-term [6]. More rapid increases in genetic resistance to sea lice through gene editing or other biotechnological approaches may be informed by investigation of closely related salmonid species demonstrating greater resistance to sea lice [16].

Coho salmon (*Oncorhynchus kitsutch*, Walbaum, 1792) demonstrate an innate ability to kill and expel sea lice. Within 24 hours of louse attachment, coho salmon mount an acute epithelial hyperplasia response associated with a thickening of the skin, inflammation, cell proliferation, and an infiltration of immune cells [17-19]. This localized swelling can even encapsulate attached lice after 10 days post exposure [17, 19] and causes 90% of lice to drop off their coho salmon hosts between 7 – 14 days post exposure [18, 20]. In contrast, minimal swelling and rapid degradation of the epidermis occurs in response to an attached louse in highly susceptible Atlantic salmon [17]. The resistance of coho salmon to sea lice has therefore been proposed to be the result of an immune and wound-healing response that is greater in magnitude and very different in character compared to that of Atlantic salmon [21, 22]. This is supported by the upregulation of multiple genes associated with inflammation, tissue remodelling, and cell adhesion in the skin of coho salmon but not Atlantic salmon in response to sea lice [22, 23]. Both Atlantic salmon and coho salmon have also been suggested to mount a nutritional immune response to sea lice [24, 25], where iron availability is limited to deter

iron-seeking pathogens [26]. However, the exact molecular and cellular mechanisms underlying coho salmon's resistance to sea lice remain elusive.

This uncertainty is in part due to the cellular heterogeneity of fish skin. The skin's multiple layers demonstrate distinct transcriptomic profiles reflecting each layer's unique composition of cell types [27]. The outermost layer of skin, the epidermis, is populated primarily by filament-filled keratinocytes [28] in three layers: an upper layer of flattened superficial keratinocytes, an intermediate layer of amorphous keratinocytes, and a lower layer of cuboidal basal keratinocytes [29, 30]. Specialized mucous cells are found individually throughout the epithelium and play an important role in maintaining skin integrity through mucus production [30, 31]. The dermal layer below contains fibroblasts, blood vessels, and chromatophores [30, 31] as well as scales in the trunk and fin rays in the fins, both maintained by osteoblasts [30, 32, 33]. Both epidermal and dermal layers are punctuated by endothelial blood vessels and neural structures [34]. Muscle and fat lie below the dermis and are not considered part of the skin [30]. There is also a variety of resident immune cells in the skin including T cells, B cells, neutrophils, dendritic cells, and macrophages [35].

The large diversity of specialised cell types present within the skin therefore poses a problem for traditional bulk transcriptomic approaches which average gene expression across all cell types within a tissue and may therefore be unable to detect biologically relevant cell-type specific differential gene expression in highly heterogeneous tissues [36]. Single nuclei RNA sequencing (snRNAseq) offers a solution to this issue by generating individual transcriptomes for thousands of individual cells [37]. Cells can be grouped based on their individual transcriptomes into distinct cell type clusters, whose identities can be ascertained from diagnostic marker genes, uniquely expressed in each cluster. These technologies allow the study of biological processes with unparalleled resolution, facilitating the comparison of the same cell type across groups or species.

The aim of this work was therefore to use snRNAseq to investigate the cell types and gene expression patterns characterizing the response to sea lice in the skin of Atlantic salmon and coho salmon. We specifically targeted the first 60 hours post infection by *L. salmonis* copepodids. This time frame has been largely unexplored from a transcriptomic perspective despite being associated with significant histological changes leading to lice rejection in coho salmon [23]. Comparing the cell type-specific responses of resistant and susceptible species to sea lice allowed us to identify cell types and molecular pathways involved in determining the mechanisms of resistance in coho salmon and to pinpoint candidate genes that could be targeted to improve sea lice resistance in Atlantic salmon aquaculture.

RESULTS:

A total of 10 and 12 snRNAseq libraries passed filtration for Atlantic salmon and coho salmon, respectively. These had over 244 million reads each, and at least 73% and 86% of those reads aligned uniquely to the genome, for Atlantic salmon and coho salmon, respectively (Table S1,S2). The final total number of cells obtained for each species was 50328 for Atlantic and 48341 for coho salmon (Table S3).

1. Cell Type Identities and Marker Genes

A total of 23 cell clusters were observed within each species, after clustering cells independently by species (Fig.1a,b). These clusters demonstrated distinct transcriptomic profiles and their inferred identities were consistent across species (Fig.1). Marker genes were frequently identical for the same cell type across species (Fig.1 c,d, see Fig.S1,S2 for dot plots of additional cell markers, Table 1 for functional relevance of all marker genes for ascribed cell type identity, Table S4,S5 for counts per cell type and sample) and highly concordant

between fin and skin tissue types (Fig.S3,S4). We identified all cell types expected in these tissues [30, 92] as well as several previously unreported cell types including a tuft-like "secretory" cell type.

The integration of samples from both species demonstrated the majority of cell types observed in each of the species-specific datasets (Fig.2 a). Two clusters of immune cells were uncovered in the combined dataset which we designated "lymphocyte" and "myeloid" given their expression of *itgae* [93] and *cd163* [94], respectively. The marker genes for each cluster of the combined dataset were often identical to those marker genes in the corresponding cluster in the species-specific dataset and always highly expressed (Fig.2 b,c,d), confirming the presence of identical cell types in the skin of Atlantic salmon and coho salmon. However, the species-specific datasets presented additional clusters and had a greater number of marker genes given more genes were used in the clustering (salmonids present a recent whole-genome duplication and the establishment of 1:1 orthologies are not straightforward, which resulted in many genes being removed when the datasets of the two species were combined). Therefore, all further analyses were conducted using the species-specific datasets, which we refer to exclusively from this point forward.

1.1 Non-Immune Cell Types

Keratinocytes were among the most abundant cell types. Three keratinocyte clusters were identified: basal keratinocytes, superficial keratinocytes and a third cluster of "intermediate keratinocytes", likely located between the former two keratinocyte layers and consistent with the three layers of keratinocytes observed in fish skin [29, 30]. Keratinocytes were abundant in all samples, but notably increased at 48h and 60h post infection only in coho salmon (Fig.1 e,f).

Other abundant cell types include fibroblasts, endothelial cells, and osteoblasts. Mucous cells were split into two clusters in coho salmon with many overlapping markers (Fig.S5,S6), but differing in their relative expression of different paralogs of *spdef* and *p2rx1* (see Fig.S2,S5,S6). Interestingly, *muc5* (associated with mucous cells, [85]) was expressed only in Atlantic salmon mucous cells (Fig.S1,S2). A "secretory" cell type was abundant in both species, and expressed tuft-cell marker genes (Table 1). Tuft cells line the epithelium of the gut and airway in mammals, and although their function is not well-characterized, they are associated with initiating immune responses (e.g., activating Th2 cells in response to helmith endoparasitism in mice) [95]. We speculate these may be a sacciform cell type, previously noted in coho salmon [20]. However, the noted absence of sacciform cells in Atlantic salmon [20], means that the location, morphology, and function of this newly identified cell type requires further investigation.

Neural crest cells were characterized by multiple pigment cell genes (Table 1) including *ltk*, which directs multipotent neural crest cell development into pigment cells in zebrafish [56], suggesting these cells are pigment cell progenitors. The detection of neural crest cells, red blood cells, and muscle cells predominately in trunk skin samples (Fig.1 e,f), is consistent with expectations of greater abundance of these cell types in the trunk skin than in the fins [30] given the potential to cut deeper into the dermal layer. Additionally, several clusters of neuronal and glial cells were observed, but most were observed in a single sample per species (Fig.1 e,f) suggesting they comprise neural structures which are present sporadically throughout the skin (e.g., peripheral axons [34], or the lateral line). Given their inconsistent presence within our samples we do not further consider the response of these cell types to sea lice, but note their potential to confound bulk RNAseq skin data.

Several cell types were identified in only one species. A small cluster of cells detected in coho salmon demonstrated a number of marker genes observed in cluster 196 "Integument-

Taste Bud" of a zebrafish cell atlas [53] (Table 1), which we refer to as "integument" cells henceforth. We speculate this cell cluster may represent a rare chemosensory cell type in coho salmon, which may also be present in Atlantic salmon but was unobserved due to its rarity (N = 93 cells in coho salmon). Fibroblasts (2) were detected in Atlantic salmon but not coho salmon and expressed *lamc1* and *col6a6* but also marker genes of the keratinocyte clusters (e.g., *itga6* and *pof1b*) (Fig.S1). A final cell cluster unique to Atlantic salmon was termed "Undifferentiated" because of its few distinctive marker genes (Fig.S1,S7).

1.2 Immune Cell Types

The immune cell marker gene *cd45* [96] was expressed in four and two clusters for Atlantic salmon and coho salmon, respectively (Fig.S8). These clusters were re-clustered to investigate for additional immune cell types expected to be present in the skin and potentially involved in sea lice response [18]. Sub-structuring within *cd45*+ cells revealed six main types of immune cells in both species: T cells, B cells, dendritic cells, neutrophils, macrophages, and monocytes (Fig.3 a,b). Myeloid and lymphocyte cells were clearly differentiated by the expression of *spi1b,* a marker for the myeloid lineage in zebrafish [39]. Marker genes for all immune cell types were consistent with the literature (Table 1) with the curious exception of the monocyte marker gene *mitfa*, typically associated with melanophores [56], suggesting these monocytes might develop into melanomacrophages known to be present in salmonid skin [19] (Fig.1 c,d, Fig.3 c,d, see Fig.S9-31 for violin plots of top marker genes).

While multiple macrophage and T cell subclusters were apparent in each species, their top marker genes were either largely overlapping among subclusters, mostly ribosomal genes, or had unknown biological relevance (Fig.S9-12,S17-19,S21-23,S25,S29-30), suggesting these are clustering artefacts or previously undescribed immune cell types. For instance, expression of *cd4* and *cd8* also did not conclusively differentiate T cell subclusters (Fig.S32), however, T

cells (5) in Atlantic salmon (Fig.S13) and T cells (4) in coho salmon (Fig.S24) expressed *gata3*, associated with Th2 cell activation [97]. Given this general lack of clear, biologically relevant expression differences within T cell and macrophage subclusters, and to maximize power for subsequent differential expression analyses (given the low numbers of cells in each T cell and macrophage subcluster, Table S6,S7) we grouped together all T cell subclusters and all macrophage subclusters for downstream analysis.

2. Common Responses to Sea Lice in Resistant and Susceptible Salmonid Species

A total of 4567 and 1799 unique genes were found to be differentially expressed between any treatment time point and the control in Atlantic salmon and coho salmon, respectively (see Fig.S33-35 for the distribution of differentially expressed genes within a given cell type, see Fig.S36,S37 for GO enrichment results). Some conserved wound-healing and immune responses to sea lice infection were detected in Atlantic salmon and coho salmon.

2.1 Wound-Healing Response to Sea Lice

Both species showed a clear activation of wound-healing mechanisms in response to the parasite in a variety of cell types (Fig.4). Upregulation of genes linked to limb development such as *pax9* [98] and *meis2* [99] were evident in keratinocytes, mucous cells, and/or fibroblasts. Genes associated with extracellular matrix integrity including *pdgfra* [100] and *col21a* [101] were upregulated in fibroblasts of both species. Another gene associated with healing of individual cells, *abr* [102], was significantly upregulated in macrophages and T cells in coho salmon and in mucous cells, keratinocytes, and T cells in Atlantic salmon. The upregulation of *agr2* observed in mucous cells of both species probably reflects an increased production of mucus in response to sea lice [103] potentially to aid in wound-healing [30, 92]. A gene previously found to be upregulated at louse attachment sites in Atlantic salmon [104],

aloxe3, was upregulated in mucous cells of both species but only significantly in Atlantic salmon. Mutations to *aloxe3* are associated with ichthyosis, a condition resulting in the build-up of skin cells [105], suggesting this gene could contribute to wound-healing-associated cell growth. Similarly, epidermal reinforcement-related genes *cldn8* [106] and *cntn1* [107] were more upregulated in Atlantic salmon. However, *bnc2*, associated with wound-healing and fibrosis [108], as well as black pigmentation [109], was upregulated earlier and more strongly in coho salmon basal keratinocytes. Similarly, *hspe2,* associated with cell proliferation and extracellular matrix strengthening [110], was upregulated in coho salmon fibroblasts but downregulated in Atlantic salmon fibroblasts. Therefore, while general wound-healing mechanisms are activated in both species, differences can be detected.

2.2 Immune Response to Sea Lice

A clear immune response was observed in both species in response to sea lice (Fig.5). Multiple paralogs of genes associated with immune cell development including *runx3* [111], *rarab* [112], and *gnai2* [113] were upregulated in response to sea lice in a variety of immune cell types including T cells, macrophages, and dendritic cells (Fig.5a). *Myo9b*, a gene associated with immune cell motility and activation [114] was upregulated in dendritic cells, neutrophils, and macrophages in both species, though showing a faster and more intense upregulation in coho salmon (Fig.5a). Major histocompatibility components were significantly upregulated in macrophages and T cells (*MHCII* only) but surprisingly in non-immune cell types too, mainly keratinocytes, and particularly superficial keratinocytes (Fig.5b). The involvement of the complement immune system was unclear. Two paralogs of *c4* were upregulated in Atlantic salmon fibroblasts while in coho salmon fibroblasts, one paralog was not differentially expressed, and the other was upregulated at 24h but downregulated at 36h and 60h (Fig.5c). C*fd* was significantly downregulated in Atlantic salmon fibroblasts but was

not significantly differentially expressed in coho salmon (Fig.5c). This is consistent with previous observations of the downregulation of this gene in Atlantic salmon in response to *L. salmonis* sea lice [104]. Though Atlantic salmon demonstrated robust activation of T cells through the significant upregulation of *cd28*, *ifit9*, *sox4* [115], *cxcr4* [116], and *ly-9* [117], they also significantly upregulated anti-inflammatory *socs3* [118] (Fig.5d).

3. Responses to Sea Lice Unique to Coho Salmon

3.1 Downregulation in Coho Salmon Red Blood Cells in Response to Sea Lice

Atlantic salmon red blood cells upregulated a number of genes associated with iron binding including several hemoglobin and ferritin subunits, and *tfr1a* [119] and other genes key to red blood cell function including s*lc4a1a* (ion transportation, [120], and *alas2* (heme biosynthesis, [25]) (Fig.6a). On the contrary, there was a significant downregulation of these genes in coho salmon red blood cells (Fig.6a). A regulation of iron in coho salmon red blood cells was further supported by the enrichment of a variety of iron-related GO terms (e.g., iron ion transport – GO:0006826) in sea louse infected samples of coho salmon but not Atlantic salmon (Fig.6b).

3.2 Keratinocytes are Key to Epithelial Hyperplasia Response to Sea Lice in Coho Salmon

Coho salmon keratinocytes exclusively significantly upregulated a variety of genes associated with epidermal re-organization (Fig.7a,b). Keratinocytes in both species were enriched for intermediate filament cytoskeleton organization (GO:0045104) and intermediate filament-based process (GO:0045103), consistent with the known abundance of filaments observed in salmon keratinocytes [28] (Fig.7c). However, the fold enrichment was much higher in coho salmon, indicating greater cell movement and restructuring of keratinocytes in this species (Fig.7c).

Coho salmon superficial keratinocytes expressed genes more associated with cell motility and immune cell localization, consistent with their location in the outermost layer of the epidermis and in direct contact with attached lice [30] (Fig.7b). The GO term epidermis development (GO:0008544) was enriched in coho salmon superficial keratinocytes and to a lesser extent in intermediate keratinocytes (Fig.7c). Increased cell motility in coho salmon superficial keratinocytes and intermediate keratinocytes was also evident by the increased expression of *glipr2*, associated with cell migration particularly in response to hypoxia [121], and *egfra*, associated with epidermal cell proliferation [122] (Fig.7a). Coho salmon superficial keratinocytes also upregulated genes related to inflammation and immune cell infiltration including: *sat1* [123], *spns2* [124], and *cdh26* [125], (Fig.7a).

In contrast, the basal keratinocyte response in coho salmon was characterized by the upregulation of genes associated with extracellular matrix reinforcement, consistent with their location in the outermost layer of the dermis [30] (Fig.7b). Genes associated with cell adhesion and the extracellular matrix including *plecb* [126] and *mmp30* [127] were significantly upregulated in coho salmon (Fig.7a). GO terms associated with extracellular matrix development (e.g., cell-cell adhesion via plasma-membrane adhesion molecules – GO:0098742, and cell adhesion – GO: 0007155, which is also enriched in intermediate keratinocytes) were also significantly enriched in coho salmon basal keratinocytes (Fig.7c). This layer of keratinocytes may also be responsible for directing the movement of upper layers of keratinocytes through the upregulation of genes known to regulate cell motility including *plekhgb5b* [128] and *quo* [129] (Fig.7a) and supported by the significant enrichment for GO: 0032231, regulation of actin filament bundle assembly (Fig.7b,c). Coho salmon basal keratinocytes also upregulated the immune gene *jak2a* (Fig.7a), which regulates hematopoiesis [130], promotes cell proliferation [131] and is inhibited by *socs3* [132] (upregulated only in Atlantic salmon (Fig.5d)). An aerolysin-like protein, which breaks down cell membranes [133]

and is upregulated in fish in response to bacterial infections [e.g., 134, 135], was also significantly upregulated exclusively in coho salmon basal keratinocytes (Fig.7a), confirming earlier observations of the upregulation of this gene exclusively in the skin of coho salmon but not of Atlantic salmon in response to sea lice [23].

The differentially expressed genes characterizing the intermediate keratinocytes response to sea lice in coho salmon largely overlapped with either the basal or superficial keratinocytes (Fig.7a). This less specialized role is consistent with their location between the superficial and basal keratinocytes. It may also reflect their recent generation from basal keratinocytes [136] as evidenced by the particular increase in abundance of this layer of keratinocytes at 48-60h (Fig.1f).

3.3 Other Cell Types Potentially Contributing to Coho Salmon Epithelial Hyperplasia in Response to Sea Lice

Several additional cell types express genes related to inflammation in coho salmon (Fig.8). Secretory cells significantly upregulate *ttc7a* from 24h onward in coho salmon but this gene was only significantly upregulated at 36h in Atlantic salmon. This gene is associated with epithelial inflammation in mice [137]. Alternatively, *mrc1*, a gene linked to inflammation [138] and associated with increased *C. rogercresseyi* sea lice count on Atlantic salmon [139], was significantly upregulated in coho salmon but not Atlantic salmon endothelial cells. Coho salmon macrophages also demonstrated upregulation of the inflammation-associated gene *usp47* [140]. Multiple cell types may therefore potentially regulate the keratinocyte epithelial hyperplasia response to sea lice observed in coho salmon.

DISCUSSION:

Our results suggest that Atlantic salmon and coho salmon skin share a common set of cell types consistent with their recent divergence 30 million years ago [141]. Many of these cell types demonstrate a clear response to sea lice, which includes the activation of wound-healing and immune mechanisms, often common to both species. Conversely, lice immunomodulation of a variety of cell types was evident only in Atlantic salmon. Additionally, the coho salmon response to sea lice presented unique signatures, characterized by iron-limitation in red blood cells and a dramatic stimulation and re-organization of keratinocytes. These processes are likely to be major contributors to the greater resistance of this species to sea lice, and the underlying genes and regulatory networks detected here are potential candidates whose expression and functioning could be disrupted to "rewire" the host response to sea lice in Atlantic salmon via biotechnological approaches such as gene editing [16].

Wound-Healing Response

Both species appear to employ a common wound-healing response to sea lice using a combination of keratinocytes, fibroblasts, mucous cells, and immune cells, in agreement with the critical role of these cell types in response to skin laceration [92]. The expression of limb development-related genes in multiple cell types also confirms a large-scale rearrangement of the skin in response to wounding [30]. Fibroblastic repair of the dermis, as expected shortly after wounding [30], was also evident through the upregulation of genes related with extracellular matrix reconstruction in fibroblasts in both species. Mucous cell upregulation of *abr2* also suggests both species increased mucus production in response to sea lice. Though sea lice feed on mucus [142], increased mucus production is a characteristic wound-healing response in Atlantic salmon [30, 92]. Alternatively, mucus upregulation may be particularly adaptive in coho salmon since, unlike Atlantic salmon, mucus of this species does not prompt

a protease increase from sea lice, suggesting coho salmon mucus may contain protective qualities [143].

Immune Response

Both species mount a common immune response to sea lice invoking the innate, adaptive, and complement immune systems. The upregulation of major histocompatibility proteins in the skin of both species is consistent with previous observations [24, 144]. However, the expression of *MHCII* in the superficial keratinocytes was surprising given that these cells are not typically associated with antigen presentation. Nonetheless, this result is consistent with and may explain previous observations of *MHCII* expression in Atlantic salmon epidermis in response to sea lice [24, 145]. Our results support the potential importance of superficial keratinocytes for sensing pathogens via antigen presentation and initiating immune and inflammatory responses [146].

Similarly, keratinocytes and fibroblasts seem to be key to the activation of the complement immune system. However, our results do not provide clear support for the importance of the complement immune response to sea lice resistance. This is consistent with previous observations of both the upregulation [139, 147] and downregulation [104] of complement proteins in Atlantic salmon in response to sea lice. Our results therefore support earlier suggestions that activation of the complement pathway may not be sufficient to grant sea lice immunity in Atlantic salmon [139].

Our results also potentially indicate that Atlantic salmon and coho salmon preferentially employ different immune cells in response to sea lice. Atlantic salmon had far more T cells than coho salmon (Fig.1e,f) perhaps as a consequence of artificial selection in this aquaculture strain of Atlantic salmon for greater disease resistance [148]. Atlantic salmon also demonstrated greater upregulation of genes associated with T cell activation. This observation

may be partly attributable to differences in power among species to detect differential expression in T cells but is consistent with previous evidence suggesting a T cell dominated response to sea lice in Atlantic salmon [149]. In contrast, coho salmon potentially show a greater use of their macrophages in response to sea lice, as evidenced by the significant enrichment for "antigen processing and presentation" (GO:0019882) in coho salmon but not Atlantic salmon macrophages. Our results also support the key role of macrophages in directing coho salmon skin inflammation in response to sea lice [17], specifically through the upregulation of *usp47* and *ndst1a*, genes which are both associated with macrophage-driven inflammation [140, 150]. We speculate that coho salmon employ a macrophage-dominant innate immune response to sea lice, while Atlantic salmon try (and fail) to employ a T cell-led adaptive immune response. More sampling or targeted snRNAsequencing of immune cells, allowing for greater power to detect cell type heterogeneity within macrophages and T cells in each species, could be helpful to test this hypothesis.

A surprising result was the seeming lack of response in neutrophils to sea lice in either species. Few differentially expressed genes were observed in this cell type and no GO terms were enriched for either species, likely a result of low power due to the few neutrophils detected in each species. This scarcity of neutrophils was itself somewhat surprising given that previous histological work has suggested increased abundance of neutrophils at the site of wound healing in both species [17]. Upregulation of genes identified in this study as markers for neutrophils (e.g., *mmp9*, *mmp13*, *csf3r*) have also been observed to be upregulated at the site of sea lice attachment in both species [e.g., 22, 151]. This discrepancy may reflect a true relative rarity of neutrophils in comparison to other skin cell types (e.g., keratinocytes and fibroblasts which dominated our samples). Alternatively, this may be a sampling bias due to the demonstrated difficulty in capturing this cell type with scRNAseq [152]. More sampling, adjustment of nuclei isolation protocols to target immune cells, or integration of

snRNAsequencing data with spatial transcriptomic data may therefore help us to learn more about what immune cells are doing in response to sea lice.

Potential Immunomodulation of Atlantic Salmon By Sea Lice

Given the known susceptibility of Atlantic salmon to sea louse immunomodulation [153, 154], differences in immune and wound-healing response between Atlantic salmon and coho salmon may not only reflect host physiological differences but also the differential capacity of sea lice to immunomodulate each species. For example, upregulation of the inflammation-dampening *socs3* [118] in Atlantic salmon may be induced by sea louse immunomodulation. This gene is also upregulated in Atlantic salmon skin and head kidney in response to *C. rogercresseyi*, but is downregulated when Atlantic salmon are fed an immunostimulatory diet associated with lower lice counts, suggesting that this upregulation in response to *C. rogercresseyi* is maladaptive [155]. *Socs* genes are commonly targeted by fish pathogens to dampen host immunity [156] and may be particularly effective at preventing macrophage activation (e.g., in turbot in response to bacterial pathogens [157]). Our results therefore suggest that *L. salmonis* induce *socs3* upregulation in Atlantic salmon in order to weaken their hosts.

Lice immunomodulation may have also caused the dampened expression of *hspe2* and *bnc2* in Atlantic salmon, potentially resulting in reduced capacity for wound-healing, and, in the case of *bnc2*, melanism [109]. Melanism is frequently observed at the louse attachment sites in Atlantic salmon [30] and is more pronounced in Atlantic salmon with more sea lice resistance [158]. Therefore, sea lice may downregulate *bnc2* in Atlantic salmon to prevent effective wound healing.

Upregulation of haemoglobin and ferritin in Atlantic salmon red blood cells could also reflect lice immunomodulation for the purposes of increasing the parasite's access to the host's

448 iron. Many pathogens manipulate iron homeostasis to increase available iron both for
449 nutritional purposes and potentially as a method of weakening their host [159, 160], as excess
450 iron can contribute to Fenton Chemistry production of harmful reactive oxygen-containing
451 species [161]. Ferritin and genes related to heme biosynthesis have previously been observed
452 to be upregulated in the skin of Atlantic salmon in response to *L. salmonis* [162]. This was
453 suggested to be an adaptive compensatory response to blood loss from *L. salmonis* parasitism,
454 however, we suggest that this may instead be a maladaptive response due to *L. salmonis*
455 immunomodulation of Atlantic salmon. This is supported by the observation that haemoglobin
456 is downregulated in Atlantic salmon infected with *C. rogercresseyi* when they are fed an
457 immunostimulatory diet [155]. *L. salmonis* secretion of prostaglandin E2 or other vasodilators
458 may underlie this response in Atlantic salmon [163]. Our results therefore suggest the potential
459 for sea lice to manipulate a wide-range of molecular pathways and phenotypes in Atlantic
460 salmon related to immune response, wound healing and iron availability. Additional molecular
461 research from the perspective of the sea louse would be useful to substantiate these findings
462 and elucidate the precise molecular strategies employed by the sea louse to elicit these
463 responses in Atlantic salmon.
464
465 *Potential Nutritional Immune Response in Coho Salmon Red Blood Cells May Discourage Sea*
466 *Lice*
467 In contrast to Atlantic salmon, coho salmon red blood cells downregulate multiple iron-
468 binding genes in response to sea lice. This could reflect differential wound-healing strategies
469 in each species or may potentially indicate an adaptive nutritional immune response.
470 Nutritional immunity, where hosts reduce the availability of iron in their tissues, is commonly
471 employed to dissuade iron-seeking pathogens [26]. Pink salmon downregulate iron-associated
472 genes in response to sea lice [164] and a nutritional immune response resulting from the

upregulation of *hepcidin 1* has been suggested for both Atlantic salmon and coho salmon [24]. However, we found low expression of hepcidin in both species in all samples. Instead, our results suggest that this nutritional immune response in coho salmon is derived from the downregulation of a variety of iron-binding genes in red blood cells.

Yet, Atlantic salmon are clearly capable of mounting a similar nutritional immune response to other pathogens. For example, plasma iron significantly decreased in Atlantic salmon exposed to live and dead *Piscirickettsia salmonis* bacteria [119]. Intriguingly, Atlantic salmon seem capable of mounting a similar nutritional immune response by upregulating genes associated with heme degradation when parasitized by *C. rogercresseyi* but not *L. salmonis* [162]. *L. salmonis*' longer co-evolutionary history with Atlantic salmon [165] may have resulted in its greater capacity to immunomodulate Atlantic salmon in comparison to *C. rogercresseyi.* Given the susceptibility of Atlantic salmon to both sea louse species, restoring Atlantic salmon's adaptive nutritional immunity may not be sufficient to confer resistance to *L. salmonis*. However, this may still result in positive animal welfare consequences given that iron limitation can prevent opportunistic microbial infections [166] that are often associated with the sites of sea lice attachment [167].

Keratinocytes Key to Coho Salmon Epithelial Hyperplasia Immune Response to Sea Lice

Our results strongly suggest that keratinocytes are responsible for the epithelial hyperplasia response characterized by filament development, inflammation, and cell proliferation that coho salmon employ to expel sea lice [17, 18, 21]. This is evidenced by our observations of a significant upregulation of genes associated with cell proliferation, cell motility, and extracellular matrix strengthening in keratinocytes, in addition to their dramatic increase in abundance during sea lice infection. However, our results further reveal keratinocytes play an active immunological role in response to sea lice. Given their capacity

for antigen presentation through the expression of *MHCII*, superficial keratinocytes may play a sentinel role in the detection of sea lice and subsequently attract immune cells to the site of an attached sea lice. Superficial keratinocytes, and to a lesser extent intermediate keratinocytes also seem to be responsible for the dramatic increase in filament cell proliferation typifying coho salmon response to sea lice [17, 18] as evidenced by their upregulation of genes related to cell motility and filament reorganization. The intermediate keratinocytes, which we suggest lie between the superficial and basal keratinocytes due to their shared marker and differentially expressed genes, rapidly increase in abundance at 48-60h post sea lice infection and are likely responsible for the observed skin thickening in coho salmon in response to sea lice [17, 18]. Basal keratinocytes, alternatively, regulate the cell motility and proliferation of the upper layers of keratinocytes, strengthen the basement membrane of the epidermis, and emit antibacterial aerolysin proteins to prevent secondary microbial infections. Therefore, each layer of keratinocytes plays a unique but integrated role in the observed epithelial hyperplasia characterising coho salmon's response to sea lice.

CONCLUSIONS:

In this study, we revealed the cell-specific mechanisms underlying responses to sea lice in a susceptible and a resistant salmonid species. Single nuclei RNA sequencing allowed us to identify the importance of genes with cell type-specific expression patterns, teasing apart cell-type specific responses, including variation in the functional roles among keratinocytes. Our results suggest a complex interplay of genes and cell types associated with sea lice response in both Atlantic salmon and coho salmon. The susceptibility of Atlantic salmon to sea lice infection despite clear activation of the complement, innate, and adaptive immune systems, confirms the insufficiency of this species immune response to effectively repel sea lice. Coho salmon, alternatively, demonstrate multiple interesting strategies in response to sea lice but

keratinocytes seem to be key to the epithelial hyperplasia underlying coho salmon sea lice resistance.

The candidate genes we identified underlying coho salmon's resistance and Atlantic salmon's susceptibility hold significant promise for enhancing sea lice resistance in Atlantic salmon via biotechnological approaches such as gene editing. Knocking out genes in Atlantic salmon that we identified as upregulated during lice infestation and potentially linked to immunodeficiency and sea lice immunomodulation through CRISPR-Cas9 editing holds the potential to significantly enhance the species' resistance to sea lice. Furthermore, promoting the expression of those genes associated with a dampened immune response in Atlantic salmon or those associated with epithelial hyperplasia in coho salmon could also effectively strengthen lice resistance in Atlantic salmon. Our findings thus offer actionable insights to mitigate the economic and ecological toll of sea lice infestations in the Atlantic salmon aquaculture industry.

METHODS:

Experimental Design

Atlantic salmon eggs with poorer than average estimated breeding values for resistance to sea lice were sourced from Benchmark Genetics Iceland. Coho salmon (1 - 2 g) were provided by the Quinsam River Hatchery, Quinsam River, BC, Canada. Both species were reared in a Recirculating Aquaculture System at the Center for Aquaculture Technologies (PEI, Canada) in freshwater until post-smolt stage (approximately 15 g), after which fish were gradually transferred to saltwater and reared to a target weight of approximately 25 g. During the experiment, fish were kept in 135 L tanks at approximately 12 °C. Triplicate tanks of each species were treated with locally-sourced (n = 49 / fish, [147]) *Lepeophtheirus salmonis*

548 copepodids and maintained for 60 hours and sampled every 12 hours. Untreated control fish
549 were maintained in parallel tanks and sampled at 36 hours into the experiment. Fish were
550 sedated before sampling with Tricaine methanesulfonate (100 mg L^{-1}), and then subjected to a
551 lethal blow to the head. Tissue samples (skin and pelvic fin), from louse attachment sites for
552 treated fish, were collected and immediately frozen in dry ice.
553
554 *Library Preparation and Sequencing*
555 Nuclei were isolated from one skin and one fin sample from each of the 5 treatment
556 timepoints (12, 24, 36, 48, and 60 hours post exposure) as well as the control for each species (N
557 = 24 tissue samples total) using a custom protocol optimized for salmon epidermis [168]. In
558 brief, approximately 45 mg tissue samples were cut with scissors in 1 mL of TST buffer for 10
559 minutes on ice before being filtered through a 40 µm Falcon™ cell strainer (Thermo Fisher
560 Scientific, catalog no. 08-771-2). A further 1 mL of TST and 3 mL of 1X PBS + BSA buffer were
561 added to each sample before centrifuging at 4°C for 5 minutes at 500 g. Samples were
562 resuspended in 1 mL 1X ST buffer filtered again through a 40 µm cell strainer, stained with
563 Hoechst 33342 Solution (Thermo Fisher Scientific, catalog no. 62249) and then nuclei integrity
564 was visually assessed using a fluorescent microscope. A disposable flow haemocytometer (C-
565 Chip Neubauer Improved (100 µm depth), NanoEnTek, catalog no. DHC-N01) was then used to
566 estimate nuclei counts.
567 Samples were processed with Chromium Next GEM Single Cell 3' Reagent Kits v3.1
568 (Dual Index) (10X Genomics) using the protocol outlined in the User Guide (CG000315 Rev C).
569 Samples were diluted with nuclease-free water to a target concentration that would recover
570 approximately 7000 nuclei in the final library. Samples were then loaded on the Chromium
571 Controller for nuclei droplet formation. After subsequent nuclei and UMI barcoding and reverse
572 transcription, resulting cDNA was then amplified, fragmented, and indexed with Truseq adapters

and Illumina sample indexes. Sequencing was performed on a NovaSeq 6000 platform (Illumina) by Azenta for approximately 220 million paired end 2x150bp reads per sample.

Genome Indexing and Read Alignment with STAR

Genome indexing and library mapping was performed with STAR (version 2.7.10a, [169, 170]). We appended the mitochondrial genome from the ENSEMBL V2 Atlantic salmon genome (Salmo_salar.ICSASG_v2.dna_rm.toplevel.fa.gz, v2, release 105, masked genome, assembly ID: GCA_000233375.4) to the ENSEMBL V3 Atlantic salmon genome (Salmo_salar.Ssal_v3.1.dna_rm.toplevel.fa.gz, v3.1, release 106, masked genome, assembly ID: GCA_905237065.2) for both the .gff and .fna files prior to indexing. For coho salmon, we appended this species mitochondrial genome (version NC_009263.1, NCBI) to the ENSEMBL V2 coho salmon genome (Oncorhynchus_kisutch.Okis_V2.dna_rm.toplevel.fa.gz, v2, release 106, masked genome, assembly ID: GCA_002021735.2) for both the .gff and .fna files prior to indexing. Prior to this concatenation, the coho salmon mitochondrial genome .gff file was manually edited to convert “CDS” annotations to “exon” annotations (consistent with the Atlantic salmon mitochondrial genome .gff file) as STAR assigns transcripts to “exon” annotations in the .gff file. gffread (v0.10.1) was used to convert .gff to .gtf files [171]. Both genomes were indexed using STAR (--runMode genomeGenerate). Each library was then mapped against its corresponding genome with the 10X V3 cell barcode whitelist (3M-february-2018.txt) and using standard parameters for single cell libraries (--soloMultiMappers Unique --soloBarcodeReadLength 28 --soloType CB_UMI_Simple --soloUMIlen 12 --soloCBwhitelist 3M-february-2018.txt --soloFeatures GeneFull --clipAdapterType CellRanger4 --outFilterScoreMin 30 --soloCBmatchWLtype 1MM_multi_Nbase_pseudocounts --soloUMIfiltering MultiGeneUMI_CR --soloUMIdedup 1MM_CR --readFilesCommand zcat --outSAMtype BAM Unsorted). The raw (unfiltered) files

598 (*genes.tsv*, *barcodes.tsv*, and *matrix.mtx*) generated for each sample were then used for
599 downstream analysis. On average, there were 300 million reads per sample with 94% of reads
600 with valid barcodes, and a 62% saturation (for more details see Fig.S38, Table S1,S2).
601
602 *Quality Control, Clustering, Integration*
603 Samples were then analysed in an R (v4) environment using Seurat (v4.1, [172]). We
604 created Seurat objects for each library after removing nuclei with less than 200 features and
605 features occurring in fewer than three nuclei. One Atlantic salmon sample (Atlantic_12h_fin)
606 retained only 60 nuclei after this initial filtration and was therefore discarded from downstream
607 analysis (Table S3). We then merged samples by species into a single Seurat object. Nuclei
608 where mtDNA features accounted for 10% or more of their total UMIs were removed (Table
609 S3, Fig.S39) before removing all mtDNA features (leaving 48608 and 39312 features
610 remaining for Atlantic salmon and coho salmon, respectively). After sub-setting the Seurat
611 object into individual samples, upper and lower thresholds for UMI and feature counts per
612 nuclei were then applied individually to each sample based on knee plot visualization. For all
613 Atlantic salmon samples, only nuclei with more than 500 UMIs but less than 6000 UMIs and
614 more than 500 features and less than 3500 features were retained (Fig.S40). For coho salmon
615 samples, a lower UMI and feature count limit of 300, 500, or 750 was applied to each sample;
616 an upper UMI limit of 2000 or 6000 was applied while an upper feature limit of 1500 or 3500
617 was applied (Fig.S41). A single Atlantic salmon sample (Atlantic_24h_fin) retained only 338
618 nuclei after this initial filtration and was therefore discarded from downstream analysis (Table
619 S3).
620 Samples were then merged again into a single Seurat object by species before splitting
621 samples again into individual sample datasets. This was done to ensure that the same features
622 were considered across samples. Counts were then normalized for each sample using the

"NormalizeData" function prior to calculating cell cycle scores using the "CellCycleScoring" function (see Tables S8,S9 for list of genes used). The "v2" SCTransform version with the glmGamPoi method (v 1.8.0, [173]) was used to normalize RNA counts for each sample, regressing out scores for the S and G2M cell cycle stages. Linear dimension reduction was conducted for each sample using the "RunPCA" function with 50 PCs. After consulting Elbowplots for each sample, a UMAP using 20 PCs was run for each sample and the "FindNeighbours" function was applied using 20 PCs, before using the "FindClusters" function with a resolution of 0.2. DoubletFinder (v 2.0.3, [174]) was then applied independently to each sample selecting pK values with the highest associated BCmvn value. We assumed a 4% doublet formation rate (based on the Chromium instrument specifications) and adjusted for homotypic doublets (see Table S3 for remaining cells per sample after doublet removal).

Samples were integrated by species using 5000 features and anchors that were identified with the "rpca" reduction method and the "FindIntegrationAnchors" function. A PCA was rerun on the integrated dataset using 50 PCs, and 30 PCs were used for subsequent UMAP generation and clustering with a resolution of 0.2 (Fig.S42a,S43a). Markers for each cluster were assessed using the logistic regression method and the FindAllMarkers function on the "SCT" assay and "data" slot, using sample ID as a latent variable to help reduce batch effects among samples. We used a pseudocount of 0.001, set a p-value threshold of 0.01, and only considered genes that were upregulated, expressed in at least 25% of all nuclei (in either of the compared groups), and demonstrated the default threshold of 0.25 X difference (log-scale) between the two compared groups.

Two clusters (0 and 4) were removed from the Atlantic salmon dataset due to low average feature/UMI counts (Fig.S42c,d). Many of the marker genes for cluster 0 were ribosomal genes, suggesting poor quality nuclei (Fig.S44). Cluster 4 was also found almost exclusively in a single sample (Atlantic_Control_skin), again suggesting it was poor quality

(Fig.S42b). Similarly, cluster 1 from the coho salmon dataset was removed for having low average feature/UMI counts and because many of its markers were ribosomal genes (Fig.S43c,d,S45). The SCTransformation was then redone for each sample based on the RNA assay as described above, and integration of samples for each species was conducted as described above using 30 PCs for UMAP generation and a resolution of 0.2 for clustering for Atlantic salmon and 20 PCs for UMAP generation and a resolution of 0.2 for clustering for coho salmon. An additional cluster (11) was subsequently removed from the coho salmon dataset for having many ribosomal marker genes (Fig.S46,S47). The SCTransformation of each sample and integration of samples was again redone for the coho salmon dataset after removing this cluster, again using 20 PCs for UMAP generation and a resolution of 0.2 for clustering. (See Table S3 for remaining cells per sample and Fig.S48 for the distribution of UMIs and features per sample after all filtering.)

Sub-clustering

Clusters identified as immune cells based on the expression (Fig.S8) of *cd45* (*ptprc*) (a marker gene for immune cells, [96]) were then considered separately for each species to investigate for the presence of additional immune cell types. For immune cells identified within Atlantic salmon samples, a PCA was rerun on the integrated assay using 10 PCs, and UMAP generation and clustering were conducted using 9 PCs and a resolution of 0.3, respectively. For coho salmon immune cells, a PCA was rerun on the integrated dataset using 20 PCs, UMAP was generated using 15 PCs and clustering was conducted using a resolution of 0.4. Marker genes comparing each immune cell cluster with all other immune cells were then identified using the same marker gene detection method described above using the "FindAllMarkers" function but UMI counts were not re-corrected based on the sub-setted datasets (recorrect_umi = FALSE). Marker genes were investigated and visualized to assess cell type. All clusters

identified as macrophages were grouped together as were all clusters identified as T-Cells (see Results).

Within a single cluster of the coho salmon dataset (cluster 12) we observed expression of the *ltk* gene (a marker of neural crest cells in Atlantic salmon, see results below) in a small subset of cells within this cluster while other cells within this cluster demonstrated expression of *casq1b* (a marker of muscle cells in Atlantic salmon, see results below) (Fig.S49a,b). To investigate the potential for multiple cell types within this cluster, we reran a PCA on cells from this cluster using the integrated assay and 10 PCs, before performing UMAP generation using 3 PCs and clustering with a resolution of 0.02. The resulting UMAP revealed two clusters of cells, one expressing *ltk*, the other expressing *casq1b* (Fig.S49c-f).

These detected subclusters were then incorporated into the larger dataset for each species including all cell types (see Fig.S50 for distribution of UMIs and features per cluster). Marker genes were then assessed for all newly identified immune cell types using the "FindAllMarkers" function (as described above) in the context of all other cell types. The top markers based on the average log 2-fold change were then considered for each cluster to assess cell type identity. Gene annotations from the ENSEMBL genome were supplemented with EntrezID (NCBI, [175]) and UniProt [176] annotations based on querying BioMart (v 2.50.3, [177]).

Differential Gene Expression Detection

We next identified genes which were differentially expressed between the control samples and each of the infection timepoints (12, 24, 36, 48, 60 hrs post infection) for both species and all cell types using the "FindMarkers" function and the default Wilcox method. We used the SCT assay and "data" slot, imposed a minimum percent threshold (percent of cells in either considered group that had to express the gene) of 0.1, set a minimum threshold p-

value of 0.01, and used the default threshold of 0.25 X difference (log-scale) between the two compared groups. We excluded results from cell types that had fewer than 50 nuclei in the control samples and comparisons where the treatment timepoint had fewer than 50 nuclei. Genes were considered differentially expressed if their adjusted p-value < 0.001. Enriched GO Biological Processes for differentially expressed genes detected for each cell type for each species were identified using ShinyGO (v 0.80, [178]). We used default parameters and limited the gene universe to all features in the RNA assay for each species (N = 48608, N = 39312 genes for Atlantic salmon and coho salmon, respectively). GO terms were considered significantly enriched if the FDR-adjusted p-value < 0.001.

Integration of Samples Across Species

We then directly compared Atlantic salmon and coho salmon samples using 6494 genes identified using Orthofinder v2.5.4 [179] as 1:1 orthologs between the two species. The transcriptomes of the Atlantic salmon and coho salmon Ensembl genomes used as reference for the snRNAseq analyses were used (Salmo_salar.Ssal_v3.1.cdna.all.fa and Oncorhynchus_kisutch.Okis_V2.cdna.all.fa). A single isoform per gene was retained using a custom python script that selects the longest transcript for each gene, and Orthofinder was run using default parameters. The orthogroups with one gene per species were considered 1:1 orthologs between Atlantic salmon and coho salmon.

Atlantic salmon and coho salmon samples were re-processed using the same quality control methods as described above, but features were winnowed down to this set of 1:1 orthologous genes just prior to the SCTransformation of individual samples. Samples from both species were then integrated together using 2000 features using anchors identified with the “rpca” reduction method with the “FindIntegrationAnchors” function. A PCA was run on the integrated dataset using 50 PCs with clustering and a UMAP was generated using 20 PCs

and a resolution of 0.2. Markers were then detected for each cluster and species using the "FindAllMarkers" function as described above. The distribution of features and UMIs as well as the top markers based on the average log 2-fold change were then considered for each cluster. A single cluster (cluster 0) was removed due to a lack of defining marker genes (Fig.S51,S52), following reclustering as above a second cluster (cluster 1) was again removed due to a lack of defining marker genes (Fig.S53,S54). After removing these clusters the SCTransformation was redone for each sample based on the RNA assay, and integration of samples for each species was conducted as described above (using 2000 features for integration, 50 PCs for the PCA, 20 PCs and a resolution of 0.2 for clustering and UMAP generation, see Fig.S55 for distribution of UMIs and features per cell type and cell type counts per sample). Markers were then detected for each cluster using the "FindAllMarkers" function as described above. The top markers based on the average log 2-fold change were then considered for each cluster to assess cell type identity.

Ethics Approval and Consent to Participate:

CATC and UPEI Animal Care Committees (AUP 21-008) approved all fish handling procedures, which were conducted in accordance with the Canadian Council for Animal Care regulations (http://www.ccac.ca/) and ARRIVE guidelines.

Consent for Publication:

Not applicable.

Availability of Data and Materials:

Sequencing data for all samples used in this study will be deposited to NCBI SRA upon article acceptance. Scripts used to analyse and visualize data are available at

748 https://github.com/SarahSalisbury/Atlantic_Salmon_vs_Coho_Salmon_Lice_Response_snR
749 NAseq.
750
751 **Competing Interests:**
752 The authors declare that they have no competing interests.
753
754 **Funding:**
755 This work was supported by FHF grant 901631 ("CrispResist"), BBSRC grant BB/V009818-
756 1 ("GenoLice") and BBSRC Institute Strategic Grants to the Roslin Institute
757 (BBS/E/D/20002172, BBS/E/D/30002275, BBS/E/D/10002070 and BBS/E/RL/230002A).
758 SJS gratefully acknowledges funding from an NSERC PDF award.
759
760 **Authors' Contributions:**
761 MDF, SJM, JEB, MDF, RDH, NR, and DR created the experimental design. MDF, RRD, and
762 DR conducted the experiment and collected tissue samples. RRD led the lab work with
763 assistance from SJS, PRV, and OG. SJS led the data analysis, interpretation, and figure
764 generation, with assistance from DR. SJS led the writing in consultation with DR and with
765 assistance from RRD, SJM, JEB, PRV, MDF, LS, RDH, and NR. All authors approved the
766 final manuscript.
767
768 **Acknowledgements:**
769 We gratefully acknowledge Paige Ackerman, Edward Walls, Sherri Higgins, Cindy Ederis for
770 contributing coho salmon from Quinsam River Hatchery as well as Ólafur H. Kristjánsson of
771 StofnFiskur, Benchmark Genetics in Iceland and Morten Rye of Benchmark Genetics in
772 Norway for contributing Atlantic salmon eggs. Our thanks go to Dr. Mark Polinksi and Russell

Anderson from FAS delivery for ensuring the safe and efficient transfer of animals; and Dr. Mark Braceland and Dr. Hiatham Mohammed from CATC, as well as Dylan Michaud for ensuring the welfare of animals throughout the experiment.

References:

1. Brooker AJ, Skern-Mauritzen R, Bron JE. Production, mortality, and infectivity of planktonic larval sea lice, *Lepeophtheirus salmonis* (Krøyer, 1837): current knowledge and implications for epidemiological modelling. ICES Journal of Marine Science. 2018; 75(4):1214-34.

2. Boxshall GA, Bravo S. On the identity of the common *Caligus* (Copepoda: Siphonostomatoida: Caligidae) from salmonid netpen systems in southern Chile. *Contributions to Zoology*. 2000;69(1-2):137-46.

3. Carvalho LA, Whyte SK, Braden LM, Purcell SL, Manning AJ, Muckle A, Fast, M. D. Impact of co-infection with *Lepeophtheirus salmonis* and *Moritella viscosa* on inflammatory and immune responses of Atlantic salmon (*Salmo salar*). Journal of fish diseases. 2020);43(4):459-73.

4. Abolofia J, Asche F, Wilen, JE. The cost of lice: quantifying the impacts of parasitic sea lice on farmed salmon. Marine Resource Economics. 2017;32(3):329-49.

5. Torrissen O, Jones S, Asche F, Guttormsen A, Skilbrei OT, Nilsen F, et al. Salmon lice–impact on wild salmonids and salmon aquaculture. Journal of fish diseases. 2013;36(3):171-94.

6. Barrett LT, Oppedal F, Robinson N, Dempster T. Prevention not cure: a review of methods to avoid sea lice infestations in salmon aquaculture. Reviews in Aquaculture. 2020;12(4):2527-43.

7. Burridge L, Weis JS, Cabello F, Pizarro J, Bostick K. Chemical use in salmon aquaculture: a review of current practices and possible environmental effects. Aquaculture. 2010;306(1-4):7-23.

8. Glover KA, Aasmundstad T, Nilsen F, Storset A, Skaala Ø. Variation of Atlantic salmon families (*Salmo salar* L.) in susceptibility to the sea lice *Lepeophtheirus salmonis* and *Caligus elongatus*. Aquaculture. 2005;245(1-4):19-30.

9. Gjerde B, Ødegård J, Thorland I. Estimates of genetic variation in the susceptibility of Atlantic salmon (*Salmo salar*) to the salmon louse *Lepeophtheirus salmonis*. Aquaculture. 2011;314(1-4):66-72.

10. Holborn MK, Rochus CM, Ang KP, Elliott JA, Leadbeater S, Powell F, Boulding EG. Family-based genome wide association analysis for salmon lice (*Lepeophtheirus salmonis*) resistance in North American Atlantic salmon using a 50 K SNP array. Aquaculture. 2019;511:734215.

11. Tsai HY, Hamilton A, Tinch AE, Guy DR, Bron JE, Taggart JB, et al. Genomic prediction of host resistance to sea lice in farmed Atlantic salmon populations. Genetics Selection Evolution. 2016;48(1):1-11.

12. Correa K, Bangera R, Figueroa R, Lhorente JP, Yáñez JM. The use of genomic information increases the accuracy of breeding value predictions for sea louse (*Caligus rogercresseyi*) resistance in Atlantic salmon (*Salmo salar*). Genetics Selection Evolution. 2017;49(1):1-5.

13. Correa K, Lhorente JP, Bassini L, López ME, Di Genova A, Maass A, et al. Genome wide association study for resistance to *Caligus rogercresseyi* in Atlantic salmon (*Salmo salar* L.) using a 50K SNP genotyping array. Aquaculture. 2017;472:61-5.

14. Rochus CM, Holborn MK, Ang KP, Elliott JA, Glebe BD, Leadbeater S, et al. Genome-wide association analysis of salmon lice (*Lepeophtheirus salmonis*) resistance in a North American Atlantic salmon population. Aquaculture Research. 2018;49(3):1329-38.

822 15. Robledo D, Gutiérrez AP, Barría A, Lhorente JP, Houston RD, Yáñez JM. Discovery and
823 functional annotation of quantitative trait loci affecting resistance to sea lice in Atlantic salmon.
824 Frontiers in genetics. 2019;10:56.
825 16. Robinson NA, Robledo D, Sveen L, Daniels RR, Krasnov A, Coates A, et al. Applying
826 genetic technologies to combat infectious diseases in aquaculture. Reviews in Aquaculture.
827 2023;15(2):491-535.
828 17. Johnson SC, Albright LJ. Comparative susceptibility and histopathology of the response of
829 naive Atlantic, chinook and coho salmon to experimental infection with *Lepeophtheirus*
830 *salmonis* (Copepoda: Caligidae). Diseases of Aquatic Organisms. 1992;14(3):179-93.
831 18. Fast MD. Fish immune responses to parasitic copepod (namely sea lice) infection.
832 Developmental & Comparative Immunology. 2014;43(2):300-12.
833 19. Braden LM, Michaud D, Groman D, Byrne P, Hori TS, Fast MD. Rejection of
834 *Lepeophtheirus salmonis* driven in part by chitin sensing is not impacted by seawater
835 acclimitization in Coho salmon (*Oncorhynchus kisutch*). Scientific Reports. 2023;13(1):1-19.
836 20. Fast MD, Sims DE, Burka JF, Mustafa A, Ross NW. Skin morphology and humoral non-
837 specific defence parameters of mucus and plasma in rainbow trout, coho and Atlantic salmon.
838 Comparative Biochemistry and Physiology Part A: Molecular & Integrative Physiology.
839 2002;132(3):645-57.
840 21. Johnson SC, Fast MD. Interactions between sea lice and their hosts. In: Wiegertjes GF, Flik
841 G. Host-Parasite Interactions. Abingdon, UK: Taylor & Francis; 2004. p. 131–59.
842 22. Valenzuela-Muñoz V, Boltaña S, Gallardo-Escárate C. Comparative immunity of *Salmo*
843 *salar* and *Oncorhynchus kisutch* during infestation with the sea louse *Caligus rogercresseyi*:
844 An enrichment transcriptome analysis. Fish & shellfish immunology. 2016;59:276-87.

845 23. Fast MD, Braden LM. Salmon-louse interaction and immunological consequences for the
846 host. In: Treasurer J, Bricknell IR, Bron JE. Sea Lice Biology and Control. Essex UK: 5M
847 Books Ltd; 2022. p. 272-93.
848 24. Braden LM, Koop BF, Jones SR. Signatures of resistance to *Lepeophtheirus salmonis*
849 include a TH2-type response at the louse-salmon interface. *Developmental & Comparative*
850 *Immunology*. 2015;48(1):178-91.
851 25. Valenzuela-Muñoz V, Boltaña S, Gallardo-Escárate C. Uncovering iron regulation with
852 species-specific transcriptome patterns in Atlantic salmon and coho salmon during a *Caligus*
853 *rogercresseyi* infestation. Journal of fish diseases. 2017;40(9):1169-84.
854 26. Murdoch CC, Skaar EP. Nutritional immunity: the battle for nutrient metals at the host–
855 pathogen interface. Nature Reviews Microbiology. 2022;20(11):657-70.
856 27. Sveen LR, Robinson N, Krasnov A, Daniels RR, Vaadal M, Karlsen C, Ytteborg E,
857 Robledo D, Salisbury S, Dagnachew B, Lazado CC. Transcriptomic landscape of Atlantic
858 salmon (*Salmo salar* L.) skin. G3. 2023:jkad215.
859 28. Hawkes JW. The structure of fish skin: I. General organization. Cell and Tissue Research.
860 1974;149(2):147-58.
861 29. Quilhac A, Sire JY. Spreading, proliferation, and differentiation of the epidermis after
862 wounding a cichlid fish, *Hemichromis bimaculatus*. The Anatomical Record: An Official
863 Publication of the American Association of Anatomists. 1999;254(3):435-51.
864 30. Sveen L, Karlsen C, Ytteborg E. Mechanical induced wounds in fish–a review on models
865 and healing mechanisms. Reviews in Aquaculture. 2020;12(4):2446-65.
866 31. Elliott, D. G. (2011). THE SKIN| Functional morphology of the integumentary system in
867 fishes. In: Farrell AP. Encyclopedia of Fish Physiology. Academic Press. p.476-88.
868 32. Elliott DG. Integumentary system. In: The laboratory fish. 2000. Academic Press. p. 271-
869 306.

870 33. Sehring IM, Weidinger G. Recent advancements in understanding fin regeneration in
871 zebrafish. Wiley Interdisciplinary Reviews: Developmental Biology. 2020;9(1):e367.
872 34. Rasmussen JP, Vo NT, Sagasti A. Fish scales dictate the pattern of adult skin innervation
873 and vascularization. Developmental cell. 2018;46(3):344-59.
874 35. Esteban MÁ, Cerezuela R. Fish mucosal immunity: skin. In: Beck BH, Peatman E. Mucosal
875 health in aquaculture. 2015. Academic Press. p. 67-92.
876 36. Chen G, Ning B, Shi T. Single-cell RNA-seq technologies and related computational data
877 analysis. Frontiers in genetics. 2019;10:317.
878 37. Kolodziejczyk AA, Kim JK, Svensson V, Marioni JC, Teichmann SA. The technology and
879 biology of single-cell RNA sequencing. Molecular cell. 2015;58(4):610-20.
880 38. Sun S, Liu Z, Jiang Q, Zou Y. Embryonic expression patterns of *TBC1D10* subfamily genes
881 in zebrafish. Gene Expression Patterns. 2022;43:119226.
882 39. Carmona SJ, Teichmann SA, Ferreira L, Macaulay IC, Stubbington MJ, Cvejic A, et al.
883 Single-cell transcriptome analysis of fish immune cells provides insight into the evolution of
884 vertebrate immune cell types. Genome research. 2017;27(3):451-61.
885 40. Raab M, Wang H, Lu Y, Smith X, Wu Z, Strebhardt K, et al. T cell receptor “inside-out”
886 pathway via signaling module *SKAP1*-RapL regulates T cell motility and interactions in lymph
887 nodes. Immunity. 2010;32(4):541-56.
888 41. Mason DY, Cordell J, Brown M, Pallesen G, Ralfkiaer E, Rothbard J, Crumpton M, Gatter
889 KC. Detection of T cells in paraffin wax embedded tissue using antibodies against a peptide
890 sequence from the *CD3* antigen. Journal of Clinical Pathology. 1989;42(11):1194-200.
891 42. Lang G, Wotton D, Owen MJ, Sewell WA, Brown MH, Mason DY, et al. The structure of
892 the human *CD2* gene and its expression in transgenic mice. The EMBO Journal.
893 1988;7(6):1675-82.

894 43. Nechanitzky R, Akbas D, Scherer S, György I, Hoyler T, Ramamoorthy S, et al.
895 Transcription factor *EBF1* is essential for the maintenance of B cell identity and prevention of
896 alternative fates in committed cells. Nature immunology. 2013;14(8):867-75.
897 44. Borggrefe T, Keshavarzi S, Gross B, Wabl M, Jessberger R. Impaired *IgE* response in
898 *SWAP-70*-deficient mice. European journal of immunology. 2001;31(8):2467-75.
899 45. Liu X, Li YS, Shinton SA, Rhodes J, Tang L, Feng H, et al. Zebrafish B cell development
900 without a pre–B cell stage, revealed by *CD79* fluorescence reporter transgenes. The Journal of
901 Immunology. 2017;199(5):1706-15.
902 46. Karsunky H, Merad M, Cozzio A, Weissman IL, Manz MG. *Flt3* ligand regulates dendritic
903 cell development from *Flt3*+ lymphoid and myeloid-committed progenitors to *Flt3*+ dendritic
904 cells in vivo. The Journal of experimental medicine. 2003 ;198(2):305-13.
905 47. Marafioti T, Paterson JC, Ballabio E, Reichard KK, Tedoldi S, Hollowood K, et al. Novel
906 markers of normal and neoplastic human plasmacytoid dendritic cells. Blood, The Journal of
907 the American Society of Hematology. 2008;111(7):3778-92.
908 48. Liu F, Wu HY, Wesselschmidt R, Kornaga T, Link DC. Impaired production and increased
909 apoptosis of neutrophils in granulocyte colony-stimulating factor receptor–deficient mice.
910 Immunity. 1996;5(5):491-501.
911 49. Taylor RS, Ruiz Daniels R, Dobie R, Naseer S, Clark TC, Henderson NC, et al. Single cell
912 transcriptomics of Atlantic salmon (*Salmo salar* L.) liver reveals cellular heterogeneity and
913 immunological responses to challenge by *Aeromonas salmonicida*. Frontiers in Immunology.
914 2022;13:984799.
915 50. Sharma A, Rijavec M, Tomar S, Yamani A, Ganesan V, Krempski J, et al. Acute systemic
916 myeloid inflammatory and stress response in severe food allergic reactions. Clinical &
917 Experimental Allergy. 2023;53(5):536-549.

51. Ito D, Kumanogoh A. The role of *Sema4A* in angiogenesis, immune responses, carcinogenesis, and retinal systems. Cell adhesion & migration. 2016;10(6):692-9.

52. Sehgal A, Donaldson DS, Pridans C, Sauter KA, Hume DA, Mabbott NA. The role of *CSF1R*-dependent macrophages in control of the intestinal stem-cell niche. Nature communications. 2018;9(1):1272.

53. Farnsworth DR, Saunders LM, Miller AC. A single-cell transcriptome atlas for zebrafish development. Developmental biology. 2020;459(2):100-8.

54. Liuzzo JP, Petanceska SS, Moscatelli D, Devi LA. Inflammatory mediators regulate cathepsin S in macrophages and microglia: a role in attenuating heparan sulfate interactions. Molecular medicine. 1999;5:320-33.

55. Anbazhagan K, Duroux-Richard I, Jorgensen C, Apparailly F. Transcriptomic network support distinct roles of classical and non-classical monocytes in human. International reviews of immunology. 2014;33(6):470-89.

56. Subkhankulova T, Camargo Sosa K, Uroshlev LA, Nikaido M, Shriever N, Kasianov AS, et al. Zebrafish pigment cells develop directly from persistent highly multipotent progenitors. Nature Communications. 2023;14(1):1258.

57. Ruhrberg C, Hajibagheri MN, Parry DA, Watt FM. Periplakin, a novel component of cornified envelopes and desmosomes that belongs to the plakin family and forms complexes with envoplakin. The Journal of cell biology. 1997;139(7):1835-49.

58. Berdyshev E, Goleva E, Bronova I, Dyjack N, Rios C, Jung J, et al. Lipid abnormalities in atopic skin are driven by type 2 cytokines. JCI insight. 2018;3(4):e98006.

59. Perez CJ, Jaubert J, Guénet JL, Barnhart KF, Ross-Inta CM, Quintanilla VC, Aubin I, et al. Two hypomorphic alleles of mouse *Ass1* as a new animal model of citrullinemia type I and other hyperammonemic syndromes. The American journal of pathology. 2010;177(4):1958-68.

943 60. Rizzolio F, Bione S, Villa A, Berti E, Cassetti A, Bulfone A, et al. Spatial and temporal
944 expression of *POF1B*, a gene expressed in epithelia. Gene expression patterns. 2007;7(4):529-
945 34.
946 61. Malaisse J, Hermant M, Hayez A, Poumay Y, Lambert de Rouvroit C. Meaning of relative
947 gene expression in multilayered cultures of epidermal keratinocytes. Experimental
948 dermatology. 2014;23(10):754-6.
949 62. Brinckmann J, Hunzelmann N, Kahle B, Rohwedel J, Kramer J, Gibson MA, et al.
950 Enhanced fibrillin-2 expression is a general feature of wound healing and sclerosis: potential
951 alteration of cell attachment and storage of *TGF-β*. Laboratory investigation. 2010;90(5):739-
952 52.
953 63. Koch M, Bohrmann B, Matthison M, Hagios C, Trueb B, Chiquet M. Large and small
954 splice variants of collagen XII: differential expression and ligand binding. The Journal of cell
955 biology. 1995;130(4):1005-14.
956 64. Usuba R, Pauty J, Soncin F, Matsunaga YT. *EGFL7* regulates sprouting angiogenesis and
957 endothelial integrity in a human blood vessel model. Biomaterials. 2019;197:305-16.
958 65. Ruppert AL, Keshavarz M, Winterberg S, Oberwinkler J, Kummer W, Schütz B. Advillin
959 is a tuft cell marker in the mouse alimentary tract. Journal of molecular histology. 2020;51:421-
960 35.
961 66. Willms RJ, Jones LO, Hocking JC, Foley E. A cell atlas of microbe-responsive processes
962 in the zebrafish intestine. Cell Reports. 2022;38(5).
963 67. Gerbe F, Sidot E, Smyth DJ, Ohmoto M, Matsumoto I, Dardalhon V, et al. Intestinal
964 epithelial tuft cells initiate type 2 mucosal immunity to helminth parasites. Nature.
965 2016;529(7585):226-30.

966 68. Middelhoff M, Nienhüser H, Valenti G, Maurer HC, Hayakawa Y, Takahashi R, et al.
967 *Prox1*-positive cells monitor and sustain the murine intestinal epithelial cholinergic niche.
968 Nature communications. 2020;11(1):111.
969 69. Song Y, Meng Z, Zhang S, Li N, Hu W, Li H. miR-4739/*ITGA10*/*PI3K* signaling regulates
970 differentiation and apoptosis of osteoblast. Regenerative Therapy. 2022;21:342-50.
971 70. Cool S, Jackson R, Pincus P, Dickinson I, Nurcombe V. Fibroblast growth factor receptor
972 4 (*FGFR4*) expression in newborn murine calvaria and primary osteoblast cultures.
973 International Journal of Developmental Biology. 2004;46(4):519-23.
974 71. Furlan S, Mosole S, Murgia M, Nagaraj N, Argenton F, Volpe P, Nori A. Calsequestrins in
975 skeletal and cardiac muscle from adult *Danio rerio*. Journal of muscle research and cell
976 motility. 2016;37:27-39.
977 72. Yoshimoto Y, Ikemoto-Uezumi M, Hitachi K, Fukada SI, Uezumi A. Methods for accurate
978 assessment of myofiber maturity during skeletal muscle regeneration. Frontiers in cell and
979 developmental biology. 2020;8:267.
980 73. Van der Loop FT, Van Eys GJ, Schaart G, Ramaekers FC. Titin expression as an early
981 indication of heart and skeletal muscle differentiation in vitro. Developmental re-organisation
982 in relation to cytoskeletal constituents. Journal of Muscle Research & Cell Motility.
983 1996;17:23-36.
984 74. Kimura T, Takehana Y, Naruse K. *pnp4a* is the causal gene of the medaka iridophore
985 mutant guanineless. G3: Genes, Genomes, Genetics. 2017;7(4):1357-63.
986 75. Santos ME, Braasch I, Boileau N, Meyer BS, Sauteur L, Böhne A, Belting HG, Affolter
987 M, Salzburger W. The evolution of cichlid fish egg-spots is linked with a cis-regulatory change.
988 Nature communications. 2014;5(1):5149.

989 76. Jang HS, Chen Y, Ge J, Wilkening AN, Hou Y, Lee HJ, Choi YR, Lowdon RF, Xing X, Li
990 D, Kaufman CK. Epigenetic dynamics shaping melanophore and iridophore cell fate in
991 zebrafish. Genome biology. 2021;22:1-18.
992 77. Yamada S, Sakakibara SI. Expression profile of the STAND protein *Nwd1* in the
993 developing and mature mouse central nervous system. Journal of Comparative Neurology.
994 2018;526(13):2099-114.
995 78. Fernandez T, Morgan T, Davis N, Klin A, Morris A, Farhi A, Lifton RP. Disruption of
996 contactin 4 (*CNTN4*) results in developmental delay and other features of 3p deletion
997 syndrome. The American Journal of Human Genetics. 2004;74(6):1286-93.
998 79. Maroilley T, Tsai MH, Mascarenhas R, Diao C, Khanbabaei M, Kaya S, Depienne C,
999 Tarailo-Graovac M, Klein KM. A novel FAME1 repeat configuration in a European family
1000 identified using a combined genomics approach. Epilepsia Open. 2023;8(2):659-65.
1001 80. Zhou Z, Peng X, Insolera R, Fink DJ, Mata M. Interleukin-10 provides direct trophic
1002 support to neurons. Journal of neurochemistry. 2009;110(5):1617-27.
1003 81. Joseph DB, Henry GH, Malewska A, Reese JC, Mauck RJ, Gahan JC, Hutchinson RC,
1004 Malladi VS, Roehrborn CG, Vezina CM, Strand DW. Single-cell analysis of mouse and human
1005 prostate reveals novel fibroblasts with specialized distribution and microenvironment
1006 interactions. The Journal of Pathology. 2021;255(2):141-54.
1007 82. He H, Suryawanshi H, Morozov P, Gay-Mimbrera J, Del Duca E, Kim HJ, et al. Single-
1008 cell transcriptome analysis of human skin identifies novel fibroblast subpopulation and
1009 enrichment of immune subsets in atopic dermatitis. Journal of Allergy and Clinical
1010 Immunology. 2020;145(6):1615-28.
1011 83. Song H, Sun W, Ye G, Ding X, Liu Z, Zhang S, et al. Long non-coding RNA expression
1012 profile in human gastric cancer and its clinical significances. Journal of translational medicine.
1013 2013;11(1):1-10.

1014 84. Park KS, Korfhagen TR, Bruno MD, Kitzmiller JA, Wan H, Wert SE, et al. *SPDEF*
1015 regulates goblet cell hyperplasia in the airway epithelium. The Journal of clinical investigation.
1016 2007;117(4):978-88.
1017 85. Ma J, Rubin BK, Voynow JA. Mucins, mucus, and goblet cells. Chest. 2018;154(1):169-
1018 76.
1019 86. Tarr PT, Edwards PA. *ABCG1* and *ABCG4* are coexpressed in neurons and astrocytes of
1020 the CNS and regulate cholesterol homeostasis through *SREBP-2*. Journal of lipid research.
1021 2008;49(1):169-82.
1022 87. Gerrits E, Giannini LA, Brouwer N, Melhem S, Seilhean D, Le Ber I, et al. Neurovascular
1023 dysfunction in GRN-associated frontotemporal dementia identified by single-nucleus RNA
1024 sequencing of human cerebral cortex. Nature neuroscience. 2022;25(8):1034-48.
1025 88. Seale P, Sabourin LA, Girgis-Gabardo A, Mansouri A, Gruss P, Rudnicki MA. *Pax7* is
1026 required for the specification of myogenic satellite cells. Cell. 2000;102(6):777-86.
1027 89. Kuo DS, Labelle-Dumais C, Gould DB. *COL4A1* and *COL4A2* mutations and disease:
1028 insights into pathogenic mechanisms and potential therapeutic targets. Human molecular
1029 genetics. 2012;21(R1):R97-110.
1030 90. Vernersson E, Khoo NK, Henriksson ML, Roos G, Palmer RH, Hallberg B.
1031 Characterization of the expression of the ALK receptor tyrosine kinase in mice. Gene
1032 Expression Patterns. 2006;6(5):448-61.
1033 91. Mo ES, Cheng Q, Reshetnyak AV, Schlessinger J, Nicoli S. Alk and Ltk ligands are
1034 essential for iridophore development in zebrafish mediated by the receptor tyrosine kinase *Ltk*.
1035 Proceedings of the National Academy of Sciences. 2017;114(45):12027-32.
1036 92. Sveen LR, Timmerhaus G, Krasnov A, Takle H, Handeland S, Ytteborg E. Wound healing
1037 in post-smolt Atlantic salmon (*Salmo salar* L.). Scientific reports. 2019;9(1):3565.

93. Uss E, Rowshani AT, Hooibrink B, Lardy NM, van Lier RA, ten Berge IJ. *CD103* is a marker for alloantigen-induced regulatory *CD8*+ T cells. The Journal of Immunology. 2006;177(5):2775-83.

94. Lau SK, Chu PG, Weiss LM. *CD163*: a specific marker of macrophages in paraffin-embedded tissue samples. American journal of clinical pathology. 2004;122(5):794-801.

95. Gerbe F, Jay P. Intestinal tuft cells: epithelial sentinels linking luminal cues to the immune system. Mucosal immunology. 2016;9(6):1353-9.

96. Rheinländer A, Schraven B, Bommhardt U. *CD45* in human physiology and clinical medicine. Immunology letters. 2018;196:22-32.

97. Zhu J, Yamane H, Cote-Sierra J, Guo L, Paul WE. *GATA-3* promotes Th2 responses through three different mechanisms: induction of Th2 cytokine production, selective growth of Th2 cells and inhibition of Th1 cell-specific factors. Cell research. 2006;16(1):3-10.

98. Mise T, Iijima M, Inohaya K, Kudo A, Wada H. Function of *Pax1* and *Pax9* in the sclerotome of medaka fish. Genesis. 2008;46(4):185-92.

99. Douglas G, Cho MT, Telegrafi A, Winter S, Carmichael J, Zackai EH, et al. De novo missense variants in MEIS2 recapitulate the microdeletion phenotype of cardiac and palate abnormalities, developmental delay, intellectual disability and dysmorphic features. American Journal of Medical Genetics Part A. 2018;176(9):1845-51.

100. Ushakumary MG, Riccetti M, Perl AK. Resident interstitial lung fibroblasts and their role in alveolar stem cell niche development, homeostasis, injury, and regeneration. Stem cells translational medicine. 2021;10(7):1021-32.

101. Chou MY, Li HC. Genomic organization and characterization of the human type XXI collagen (*COL21A1*) gene. Genomics. 2002;79(3):395-401.

102. Vaughan EM, Miller AL, Hoi-Ying EY, Bement WM. Control of local Rho GTPase crosstalk by *Abr*. Current biology. 2011;21(4):270-7.

1063 103. Bergström JH, Berg KA, Rodríguez-Piñeiro AM, Stecher B, Johansson ME, Hansson GC.
1064 *AGR2*, an endoplasmic reticulum protein, is secreted into the gastrointestinal mucus. PLoS
1065 One. 2014;9(8):e104186.
1066 104. Umasuthan N, Xue X, Caballero-Solares A, Kumar S, Westcott JD, Chen Z, et al.
1067 Transcriptomic profiling in fins of Atlantic salmon parasitized with sea lice: Evidence for an
1068 early imbalance between chalimus-induced immunomodulation and the host's defense
1069 response. International journal of molecular sciences. 2020;21(7):2417.
1070 105. Ullah R, Ansar M, Durrani ZU, Lee K, Santos-Cortez RL, Muhammad D, et al. Novel
1071 mutations in the genes *TGM 1* and *ALOXE 3* underlying autosomal recessive congenital
1072 ichthyosis. International journal of dermatology. 2016;55(5):524-30.
1073 106. Zeissig S, Bürgel N, Günzel D, Richter J, Mankertz J, Wahnschaffe U, et al. Changes in
1074 expression and distribution of claudin 2, 5 and 8 lead to discontinuous tight junctions and
1075 barrier dysfunction in active Crohn's disease. Gut. 2007;56(1):61-72.
1076 107. Houreld NN, Ayuk SM, Abrahamse H. Cell adhesion molecules are mediated by
1077 photobiomodulation at 660 nm in diabetic wounded fibroblast cells. Cells. 2018 Apr
1078 16;7(4):30.
1079 108. Bobowski-Gerard M, Boulet C, Zummo FP, Dubois-Chevalier J, Gheeraert C, Bou Saleh
1080 M, et al. Functional genomics uncovers the transcription factor *BNC2* as required for
1081 myofibroblastic activation in fibrosis. Nature Communications. 2022;13(1):5324.
1082 109. Patterson LB, Parichy DM. Interactions with iridophores and the tissue environment
1083 required for patterning melanophores and xanthophores during zebrafish adult pigment stripe
1084 formation. PLoS genetics. 2013;9(5):e1003561.
1085 110. Peretti T, Waisberg J, Mader AM, de Matos LL, da Costa RB, Conceição GM, et al.
1086 Heparanase-2, syndecan-1, and extracellular matrix remodeling in colorectal carcinoma.
1087 European journal of gastroenterology & hepatology. 2008;20(8):756-65.

111. Puig-Kröger A, Corbí A. *RUNX3*: a new player in myeloid gene expression and immune response. Journal of cellular biochemistry. 2006;98(4):744-56.

112. Raverdeau M, Mills KH. Modulation of T cell and innate immune responses by retinoic acid. The Journal of Immunology. 2014;192(7):2953-8.

113. Han SB, Moratz C, Huang NN, Kelsall B, Cho H, Shi CS, et al. *Rgs1* and *Gnai2* regulate the entrance of B lymphocytes into lymph nodes and B cell motility within lymph node follicles. Immunity. 2005;22(3):343-54.

114. Maravillas-Montero JL, Santos-Argumedo L. The myosin family: unconventional roles of actin-dependent molecular motors in immune cells. Journal of leukocyte biology. 2012;91(1):35-46.

115. Kuwahara M, Yamashita M, Shinoda K, Tofukuji S, Onodera A, Shinnakasu R, et al. The transcription factor *Sox4* is a downstream target of signaling by the cytokine *TGF-β* and suppresses TH2 differentiation. Nature immunology. 2012;13(8):778-86.

116. Kumar A, Humphreys TD, Kremer KN, Bramati PS, Bradfield L, Edgar CE, Hedin KE. *CXCR4* physically associates with the T cell receptor to signal in T cells. Immunity. 2006;25(2):213-24.

117. Mathieson BJ, Sharrow SO, Bottomly K, Fowlkes BJ. *Ly 9*, an alloantigenic marker of lymphocyte differentiation. Journal of immunology. 1980;125(5):2127-36.

118. Carow B, Rottenberg ME. *SOCS3*, a major regulator of infection and inflammation. Frontiers in immunology. 2014;5:58.

119. Martínez D, Oyarzún-Salazar R, Quilapi AM, Coronado J, Enriquez R, Vargas-Lagos C, et al. Live and inactivated *Piscirickettsia salmonis* activated nutritional immunity in Atlantic salmon (*Salmo salar*). Frontiers in Immunology. 2023;14:1187209.

120. Jennings ML. Cell physiology and molecular mechanism of anion transport by erythrocyte band 3/AE1. American Journal of Physiology-Cell Physiology. 2021;321(6):C1028-59.

121. Huang SG, Zhang LL, Niu Q, Xiang GM, Liu LL, Jiang DN, et al. Hypoxia promotes epithelial-mesenchymal transition of hepatocellular carcinoma cells via inducing *GLIPR-2* expression. PloS one. 2013;8(10):e77497.

122. Wee P, Wang Z. Epidermal growth factor receptor cell proliferation signaling pathways. Cancers. 2017;9(5):52.

123. Mou Y, Zhang L, Liu Z, Song X. Abundant expression of ferroptosis-related *SAT1* is related to unfavorable outcome and immune cell infiltration in low-grade glioma. BMC cancer. 2022;22(1):1-15.

124. Chen J, Ingham N, Kelly J, Jadeja S, Goulding D, Pass J, et al. Spinster homolog 2 (*spns2*) deficiency causes early onset progressive hearing loss. PLoS genetics. 2014;10(10):e1004688.

125. Caldwell JM, Collins MH, Kemme KA, Sherrill JD, Wen T, Rochman M, et al. Cadherin 26 is an alpha integrin-binding epithelial receptor regulated during allergic inflammation. Mucosal immunology. 2017;10(5):1190-201.

126. Wiche G. Commentary: Role of plectin in cytoskeleton organization and dynamics. Journal of cell science. 1998;111(17):2477-86.

127. Granadeiro L, Dirks RP, Ortiz-Delgado JB, Gavaia PJ, Sarasquete C, Laize V, et al. Warfarin-exposed zebrafish embryos resembles human warfarin embryopathy in a dose and developmental-time dependent manner–From molecular mechanisms to environmental concerns. Ecotoxicology and environmental safety. 2019;181:559-71.

128. Qian M, Chen Z, Wang S, Guo X, Zhang Z, Qiu W, et al. *PLEKHG5* is a novel prognostic biomarker in glioma patients. International Journal of Clinical Oncology. 2019;24:1350-8.

129. Daggett DF, Boyd CA, Gautier P, Bryson-Richardson RJ, Thisse C, Thisse B, et al. Developmentally restricted actin-regulatory molecules control morphogenetic cell movements in the zebrafish gastrula. Current Biology. 2004;14(18):1632-8.

130. Ma AC, Ward AC, Liang R, Leung AY. The role *of jak2a* in zebrafish hematopoiesis. Blood, The Journal of the American Society of Hematology. 2007;110(6):1824-30.

131. Wu H, Huang M, Cao P, Wang T, Shu Y, Liu P. MiR-135a targets *JAK2* and inhibits gastric cancer cell proliferation. Cancer biology & therapy. 2012;13(5):281-8.

132. Sasaki A, Yasukawa H, Shouda T, Kitamura T, Dikic I, Yoshimura A. *CIS3*/*SOCS-3* suppresses erythropoietin (*EPO*) signaling by binding the *EPO* receptor and *JAK2*. Journal of Biological Chemistry. 2000;275(38):29338-47.

133. Podobnik M, Kisovec M, Anderluh G. Molecular mechanism of pore formation by aerolysin-like proteins. Philosophical Transactions of the Royal Society B: Biological Sciences. 2017;372(1726):20160209.

134. Chen LL, Xie J, Cao DD, Jia N, Li YJ, Sun H, et al. The pore-forming protein Aep1 is an innate immune molecule that prevents zebrafish from bacterial infection. Developmental & Comparative Immunology. 2018;82:49-54.

135. Xiong Y, Dan C, Ren F, Su Z, Zhang Y, Mei J. Proteomic profiling of yellow catfish (*Pelteobagrus fulvidraco*) skin mucus identifies differentially-expressed proteins in response to *Edwardsiella ictaluri* infection. Fish & Shellfish Immunology. 2020;100:98-108.

136. Lee RT, Asharani PV, Carney TJ. Basal keratinocytes contribute to all strata of the adult zebrafish epidermis. PloS one. 2014;9(1):e84858.

137. Leclerc-Mercier S, Lemoine R, Bigorgne AE, Sepulveda F, Leveau C, Fischer A, et al. Ichthyosis as the dermatological phenotype associated with *TTC7A* mutations. British Journal of Dermatology. 2016;175(5):1061-4.

138. Subramanian K, Neill DR, Malak HA, Spelmink L, Khandaker S, Marchiori GDL, et al. Pneumolysin binds to the mannose receptor C type 1 (*MRC-1*) leading to anti-inflammatory responses and enhanced pneumococcal survival. Nature microbiology. 2019;4(1):62-70.

1161 139. Robledo D, Gutiérrez AP, Barría A, Yáñez JM, Houston RD. Gene expression response
1162 to sea lice in Atlantic salmon skin: RNA sequencing comparison between resistant and
1163 susceptible animals. Frontiers in genetics. 2018;9:287.
1164 140. Palazón-Riquelme P, Worboys JD, Green J, Valera A, Martín-Sánchez F, Pellegrini C,
1165 Brough D, López-Castejón G. *USP7* and *USP47* deubiquitinases regulate *NLRP3*
1166 inflammasome activation. EMBO reports. 2018;19(10):e44766.
1167 141. Lecaudey LA, Schliewen UK, Osinov AG, Taylor EB, Bernatchez L, Weiss SJ. Inferring
1168 phylogenetic structure, hybridization and divergence times within Salmoninae (Teleostei:
1169 Salmonidae) using RAD-sequencing. Molecular phylogenetics and evolution. 2018;124:82-99.
1170 142. Pike AW. Sea lice—major pathogens of farmed Atlantic salmon. Parasitology today.
1171 1989;5(9):291-7.
1172 143. Fast MD, Burka JF, Johnson SC, Ross NW. Enzymes released from *Lepeophtheirus*
1173 *salmonis* in response to mucus from different salmonids. Journal of Parasitology. 2003;89(1):7-
1174 13.
1175 144. Fast MD, Muise DM, Easy RE, Ross NW, Johnson SC. The effects of *Lepeophtheirus*
1176 *salmonis* infections on the stress response and immunological status of Atlantic salmon (*Salmo*
1177 *salar*). Fish & Shellfish Immunology. 2006;21(3):228-41.
1178 145. Holm HJ, Skugor S, Bjelland AK, Radunovic S, Wadsworth S, Koppang EO, Evensen Ø.
1179 Contrasting expression of immune genes in scaled and scaleless skin of Atlantic salmon
1180 infected with young stages of *Lepeophtheirus salmonis*. Developmental & Comparative
1181 Immunology. 2017;67:153-65.
1182 146. Barker JN, Griffiths CE, Nickoloff BJ, Mitra RS, Dixit VM. Keratinocytes as initiators of
1183 inflammation. The Lancet. 1991;337(8735):211-4.
1184 147. Cai W, Kumar S, Navaneethaiyer U, Caballero-Solares A, Carvalho LA, Whyte SK, et al.
1185 Transcriptome analysis of Atlantic salmon (*Salmo salar*) skin in response to sea lice and

infectious Salmon Anemia Virus co-infection under different experimental functional diets. Frontiers in Immunology. 2022;12. doi:https://doi.org/10.3389/fimmu.2021.787033.

148. Robinson NA, Gjedrem T, Quillet E. Improvement of disease resistance by genetic methods. In: Jeney G. Fish diseases. Academic Press; 2017. p. 21-50

149. Skugor S, Glover KA, Nilsen F, Krasnov A. Local and systemic gene expression responses of Atlantic salmon (*Salmo salar* L.) to infection with the salmon louse (*Lepeophtheirus salmonis*). BMC genomics. 2008;9:1-18.

150. Swart M, Troeberg L. Effect of polarization and chronic inflammation on macrophage expression of heparan sulfate proteoglycans and biosynthesis enzymes. Journal of Histochemistry & Cytochemistry. 2019;67(1):9-27.

151. Øvergård AC, Eichner C, Nuñez-Ortiz N, Kongshaug H, Borchel A, Dalvin S. Transcriptomic and targeted immune transcript analyses confirm localized skin immune responses in Atlantic salmon towards the salmon louse. Fish & Shellfish Immunology. 2023;138:108835.

152. Wang L, Liu Y, Dai Y, Tang X, Yin T, Wang C, et al. Single-cell RNA-seq analysis reveals *BHLHE40*-driven pro-tumour neutrophils with hyperactivated glycolysis in pancreatic tumour microenvironment. Gut. 2023;72(5):958-71.

153. Fast MD, Johnson SC, Eddy TD, Pinto D, Ross NW. *Lepeophtheirus salmonis* secretory/excretory products and their effects on Atlantic salmon immune gene regulation. Parasite immunology. 2007;29(4):179-89.

Braden LM, Monaghan SJ, Fast MD. Salmon immunological defence and interplay with the modulatory capabilities of its ectoparasite *Lepeophtheirus salmonis*. Parasite Immunology. 2020;42(8):e12731.

154. Braden LM, Monaghan SJ, Fast MD. Salmon immunological defence and interplay with the modulatory capabilities of its ectoparasite *Lepeophtheirus salmonis*. Parasite Immunology. 2020;42(8):e12731.

155. Núñez-Acuña G, Gonçalves AT, Valenzuela-Munoz V, Pino-Marambio J, Wadsworth S, Gallardo-Escárate C. Transcriptome immunomodulation of in-feed additives in Atlantic salmon *Salmo salar* infested with sea lice *Caligus rogercresseyi*. Fish & shellfish immunology. 2015;47(1):450-60.

156. Wang T, Gorgoglione B, Maehr T, Holland JW, Vecino JL, Wadsworth S, Secombes CJ. Fish suppressors of cytokine signaling (SOCS): gene discovery, modulation of expression and function. Journal of signal transduction. 2011;905813.

157. Zhang M, Xiao ZZ, Sun L. Suppressor of cytokine signaling 3 inhibits head kidney macrophage activation and cytokine expression in *Scophthalmus maximus*. Developmental & Comparative Immunology. 2011;35(2):174-81.

158. Kittilsen S, Johansen IB, Braastad BO, Øverli Ø. Pigments, parasites and personalitiy: towards a unifying role for steroid hormones? PloS one. 2012;7(4):e34281.

159. Weinberg ED. Iron availability and infection. Biochimica et Biophysica Acta (BBA)-General Subjects. 2009;1790(7):600-5.

160. Ganz T, Nemeth E. Iron homeostasis in host defence and inflammation. Nature Reviews Immunology. 2015;15(8):500-10.

161. Drakesmith H, Prentice A. Viral infection and iron metabolism. Nature Reviews Microbiology. 2008;6(7):541-52.

162. Valenzuela-Muñoz V, Gallardo-Escárate C. Iron metabolism modulation in Atlantic salmon infested with the sea lice *Lepeophtheirus salmonis* and *Caligus rogercresseyi*: A matter of nutritional immunity? Fish & shellfish immunology. 2017;60:97-102.

1233 163. Fast MD, Ross NW, Craft CA, Locke SJ, MacKinnon SL, Johnson SC. *Lepeophtheirus*
1234 *salmonis*: characterization of prostaglandin E2 in secretory products of the salmon louse by
1235 RP-HPLC and mass spectrometry. Experimental parasitology. 2004;107(1-2):5-13.
1236 164. Sutherland BJ, Koczka KW, Yasuike M, Jantzen SG, Yazawa R, Koop BF, Jones SR.
1237 Comparative transcriptomics of Atlantic *Salmo salar*, chum *Oncorhynchus keta* and pink
1238 salmon *O. gorbuscha* during infections with salmon lice *Lepeophtheirus salmonis*. BMC
1239 genomics. 2014;15:1-17.
1240 165. Burka JF, Fast MD, Revie CW. *Lepeophtheirus salmonis* and *Caligus rogercresseyi*. In:
1241 Woo PTK, Buchmann K. Fish parasites: Pathobiology and protection. Wallingford UK: Cabi;
1242 2012. p. 350-70.
1243 166. Sheldon JR, Skaar EP. Metals as phagocyte antimicrobial effectors. Current Opinion in
1244 Immunology. 2019;60:1-9.
1245 167. Caballero-Solares A, Umasuthan N, Xue X, Katan T, Kumar S, Westcott JD, et al.
1246 Interacting Effects of Sea Louse (*Lepeophtheirus salmonis*) Infection and Formalin-Killed
1247 *Aeromonas salmonicida* on Atlantic Salmon Skin Transcriptome. Frontiers in Immunology.
1248 2022;13. doi:https://doi.org/10.3389/fimmu.2022.804987.
1249 168. Ruiz Daniels R, Taylor RS, Dobie R, Salisbury S, Furniss JJ, Clark E, Macqueen DJ,
1250 Robledo D. A versatile nuclei extraction protocol for single nucleus sequencing in non-model
1251 species–Optimization in various Atlantic salmon tissues. Plos one. 2023;18(9):e0285020.
1252 169. Dobin A. STAR manual 2.7. 0a. Weill Cornell Medicine. 2019.
1253 170. Kaminow B, Yunusov D, Dobin A. STARsolo: accurate, fast and versatile
1254 mapping/quantification of single-cell and single-nucleus RNA-seq data. Biorxiv. 2021.
1255 doi:10.1101/2021.05.05.442755.
1256 171. Pertea G, Pertea M. GFF utilities: GffRead and GffCompare. F1000Research.
1257 2020;9:ISCB Comm J-304.

1258 172. Hao Y, Hao S, Andersen-Nissen E, Mauck WM, Zheng S, Butler A, et al. Integrated
1259 analysis of multimodal single-cell data. Cell. 2021;184(13):3573-87.
1260 173. Ahlmann-Eltze C, Huber W. glmGamPoi: fitting Gamma-Poisson generalized linear
1261 models on single cell count data. Bioinformatics. 2020;36(24):5701-2.
1262 174. McGinnis CS, Murrow LM, Gartner ZJ. DoubletFinder: doublet detection in single-cell
1263 RNA sequencing data using artificial nearest neighbors. Cell systems. 2019;8(4):329-37.
1264 175. Maglott D, Ostell J, Pruitt KD, Tatusova T. Entrez Gene: gene-centered information at
1265 NCBI. Nucleic acids research. 2005;33(suppl_1):D54-8.
1266 176. UniProt Consortium. UniProt: a worldwide hub of protein knowledge. Nucleic acids
1267 research. 2019;47(D1):D506-15.
1268 177. Smedley D, Haider S, Ballester B, Holland R, London D, Thorisson G, Kasprzyk A.
1269 BioMart–biological queries made easy. BMC genomics. 2009;10(1):1-12.
1270 178. Ge SX, Jung D, Yao R. ShinyGO: a graphical gene-set enrichment tool for animals and
1271 plants. Bioinformatics. 2020;36(8):2628-9.
1272 179. Emms DM, Kelly S. OrthoFinder: phylogenetic orthology inference for comparative
1273 genomics. Genome biology. 2019;20:1-14.

Table 1 Marker genes for cell types found in skin and fin samples of Atlantic salmon and coho salmon. All noted genes were significantly ($p << 0.001$) upregulated in the given species' cell type cluster relative to all other cells.

		Cell Type	Marker Gene	Atlantic Salmon ENSEMBL ID	Coho Salmon ENSEMBL ID	Support for Cell Type Identity
Both Species		T Cells	*tbc1d10c*	ENSSSAG00000055420	ENSOKIG00005011012	Expressed in T cells [38]
			bcl11b	ENSSSAG00000071984	ENSOKIG00005023187	Expressed in T cells [39]
				ENSSSAG00000045088		
			tcf7	ENSSSAG00000006857	ENSOKIG00005033777	Expressed in T cells [39]
			skap1	ENSSSAG00000066533	ENSOKIG00005050132	Expressed in T cells [40]
			cd3	ENSSSAG00000076824		Marker for T cells [41]
			cd2		ENSOKIG00005012541	Marker for T cells [42]
		B Cells	*ebf1*	ENSSSAG00000079780	ENSOKIG00005001939	Marker for B cells [43]
				ENSSSAG00000070298		
			swap70	ENSSSAG00000115076	ENSOKIG00005020004	Marker for B cells [44]
			cd79	ENSSSAG00000113980	ENSOKIG00005014962	Marker for B cells [45]
		Dendritic Cells	*flt3*	ENSSSAG00000009390	ENSOKIG00005021723	Marker for dendritic cells [46]
				ENSSSAG00000060395		
			blnk	ENSSSAG00000023874		Expressed in dendritic cells [47]
		Neutrophils	*csf3r*	ENSSSAG00000072535	ENSOKIG00005018820	Expressed in neutrophils [48]
			mmp9	ENSSSAG00000069874		Marker for neutrophils in Atlantic Salmon [49]
			mmp13	ENSSSAG00000070495		Marker for neutrophils in Atlantic Salmon [49]
			clec4e		ENSOKIG00005020977	Expressed in neutrophils [50]
		Macrophages	*sema4ab*	ENSSSAG00000056722	ENSOKIG00005023500	Expressed in macrophages [51]
			csf1r	ENSSSAG00000047020		Expressed in macrophages [52]
				ENSSSAG00000061479		
			marco	ENSSSAG00000063051		Marker gene for macrophages in zebrafish cell atlas [53]
			ctss1		ENSOKIG00005022279	Expressed in macrophages [54]
		Monocyte	*ckb*	ENSSSAG00000003466	ENSOKIG00005016475	Expressed in monocytes [55]
			mitfa	ENSSSAG00000077659	ENSOKIG00005012208	Associated with melanophores [56]
			csf1r	ENSSSAG00000047020		
		Superficial Keratinocytes	*evpla*	ENSSSAG00000048370	ENSOKIG00005025303	Expressed in mouse suprabasal keratinocytes [57]
			ppl	ENSSSAG00000003101	ENSOKIG00005024627	Expressed in mouse suprabasal keratinocytes [57]
			elovl6	ENSSSAG00000074658	ENSOKIG00005006494	Facilitates lipid metabolism in human skin keratinocytes [58]
		Intermediate Keratinocytes	*ass1*	ENSSSAG00000053906	ENSOKIG00005029918	Expressed in mouse keratinocytes [59]
			pof1b	ENSSSAG00000040788	ENSOKIG00005024403	Expressed in human keratinocytes [60]
		Basal Keratinocytes	*itga6*	ENSSSAG00000006725	ENSOKIG00005047168	Expressed in basal epidermal cells in humans [61]
			lamb4	ENSSSAG00000106537	ENSOKIG00005007077	Marker for "fin basal cells" in zebrafish cell atlas [53]
		Fibroblasts (1)	*fbn2b*	ENSSSAG00000057875	ENSOKIG00005007419	Associated with fibroblast-driven wound healing in humans [62]
			col12a1	ENSSSAG00000070858	ENSOKIG00005043212	Expressed in the fibroblasts of chick skin [63]
		Endothelial	*egfl7*	ENSSSAG00000083641	ENSOKIG00005048982	Associated with endothelial development – specifically blood vessels [64]

			tie1	ENSSSAG00000079214	ENSOKIG00005004729	Marker for the blood vessel cell type in zebrafish cell atlas [53]
			flt4	ENSSSAG00000084309	ENSOKIG00005035303	Marker for the the blood vessel cell type in zebrafish cell atlas [53]
		Secretory	*pcdh11*	ENSSSAG00000057824	ENSOKIG00005037957	
			avil	ENSSSAG00000084911	ENSOKIG00005031571	Associated with tuft cells [65] and expressed in a rare tuft cell-like group of cells within zebrafish intestine [66]
			pou2f3	ENSSSAG00000039114	ENSOKIG00005026363	Associated with tuft cells [67] and expressed in a rare tuft cell-like group of cells within zebrafish intestine [66]
			prox1	ENSSSAG00000039610	ENSOKIG00005019222	Associated with tuft cells [68]
		Osteoblasts	*panx3*	ENSSSAG00000068856	ENSOKIG00005040175	Marker for osteoblasts in zebrafish cell atlas [53]
			itga10	ENSSSAG00000119547	ENSOKIG00005041776	Associated with bone development [69]
			fgfr4	ENSSSAG00000017777	ENSOKIG00005032151	Expressed in mouse osteoblasts [70], marker for bone in Atlantic Salmon [27]
		Red Blood Cells	*hemoglobin subunit beta*	ENSSSAG00000045065	ENSOKIG00005024058	Key component of red blood cells
		Muscle	*casq1b*	ENSSSAG00000072101	ENSOKIG00005004600	Expressed in zebrafish skeletal muscle [71]
			tnni2a	ENSSSAG00000055259	ENSOKIG00005033031	Critical to muscle function [72]
			ttn	ENSSSAG00000119643		A crucial component of skeletal muscle function [73]
				ENSSSAG00000095939		
		Neural Crest Cells	*ltk*	ENSSSAG00000110394	ENSOKIG00005047857	Directs multipotent neural crest cell development into pigment cells in zebrafish [56]
			mlphb	ENSSSAG00000053095	ENSOKIG00005009265	Marker gene for xanthophores and melanophores in zebrafish cell atlas [53]
			pnp4a	ENSSSAG00000044409	ENSOKIG00005022133	Expressed in iridophores [74]
			fhl2	ENSSSAG00000080837	ENSOKIG00005031455	Expressed in iridophores [75]
					ENSOKIG00005012190	
			alx4b	ENSSSAG00000112316	ENSOKIG00005008266	Expressed in iridophores [76]
		Neuronal (1)	*nwd1*	ENSSSAG00000047318	ENSOKIG00005015132	Associated with neuron development in mice [77]
			cntn4	ENSSSAG00000057173	ENSOKIG00005044284	Associated with neuron development in humans [78]
		Neuronal (2)	*samd12*	ENSSSAG00000118720	ENSOKIG00005014439	Linked to neurological disease in humans [79]
			il10rb	ENSSSAG00000038884	ENSOKIG00005025589	Expressed in neurons [80]
Atlantic Salmon Only		Fibroblasts (2)	*lamc1*	ENSSSAG00000008380		Expressed in mouse fibroblasts [81]
			col6a6	ENSSSAG00000040824		Expressed in human skin fibroblasts [82]
		Mucous	*fer1l4*	ENSSSAG00000075250		lncRNA associated with gastric cancer [83]
			spdef	ENSSSAG00000074163		Critical to mucus cell differentiation [84]
			p2rx1	ENSSSAG00000039817		Marker for mucus cells in zebrafish cell atlas [53]
			muc5bl	ENSSSAG00000055014		Associated with mucus cells [85]
		Glial (1)	*abcg1*	ENSSSAG00000074633		Expressed in glial but also neuronal cells [86]
		Glial (2)	*wdr49*	ENSSSAG00000064639		Associated with astrocytes [87]
		Undifferentiated	*pax7l*	ENSSSAG00000006052		Associated with myoskeleton [88]

			col4a1	ENSSSAG00000029801		Widely expressed in basement membrane [89]
Coho Salmon Only		Mucous (1)	*fer1l4*		ENSOKIG00005027833	lncRNA associated with gastric cancer [83]
			spdef		ENSOKIG00005000031	Critical to mucus cell differentiation [84]
			p2rx1		ENSOKIG00005008860	Marker for mucus cells in zebrafish cell atlas [53]
					ENSOKIG00005028810	
		Mucous (2)	*fer1l4*		ENSOKIG00005027833	lncRNA associated with gastric cancer [83]
			spdef		ENSOKIG00005003413	Critical to mucus cell differentiation [84]
			p2rx1		ENSOKIG00005028810	Marker for mucus cells in zebrafish cell atlas [53]
		Integument	*plcb2*		ENSOKIG00005013873	Marker for “Integument – taste bud” cell type in zebrafish cell atlas [53]
			rgs1		ENSOKIG00005032617	Marker for “Integument – taste bud” cell type in zebrafish cell atlas [53]
					ENSOKIG00005021878	Marker for “Integument – taste bud” cell type in zebrafish cell atlas [53]
			trpm5		ENSOKIG00005033333	Marker for “Integument – taste bud” cell type in zebrafish cell atlas [53]
			kcnk17		ENSOKIG00005039197	Marker for “Integument – taste bud” cell type in zebrafish cell atlas [53]
		Neuronal (3)	*alk*		ENSOKIG00005020768	A widely-expressed neuronal-related gene [90], also associated with pigmentation in fish [91]
		Glial	*abcg1*		ENSOKIG00005034390	Expressed in glial but also neuronal cells [86]
			wdr95		ENSOKIG00005007677	An ortholog of WDR49, which is associated with astrocytes [87]

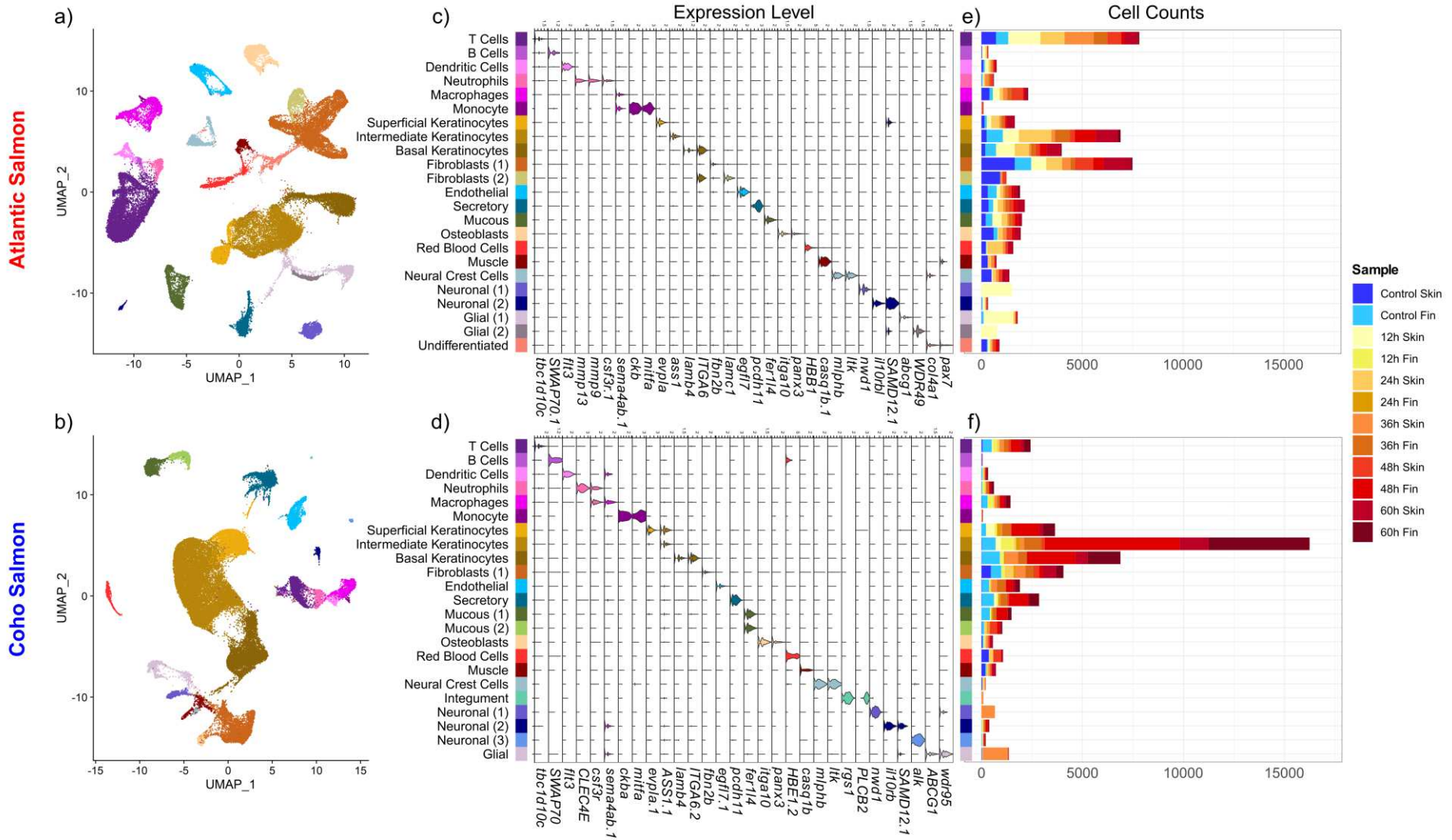

Fig.1 Cell types detected in Atlantic (a-c) and Coho (d-f) Salmon. UMAPs of cell clusters coloured by putative identity for (a) Atlantic salmon and (b) coho salmon. Violin Plots of marker genes for each cell cluster for (c) Atlantic salmon and (d) Coho Salmon. Counts of each cell type by sample for (e) Atlantic salmon and (f) coho salmon. Note there is no 12h Fin or 24h Fin sample for Atlantic salmon.

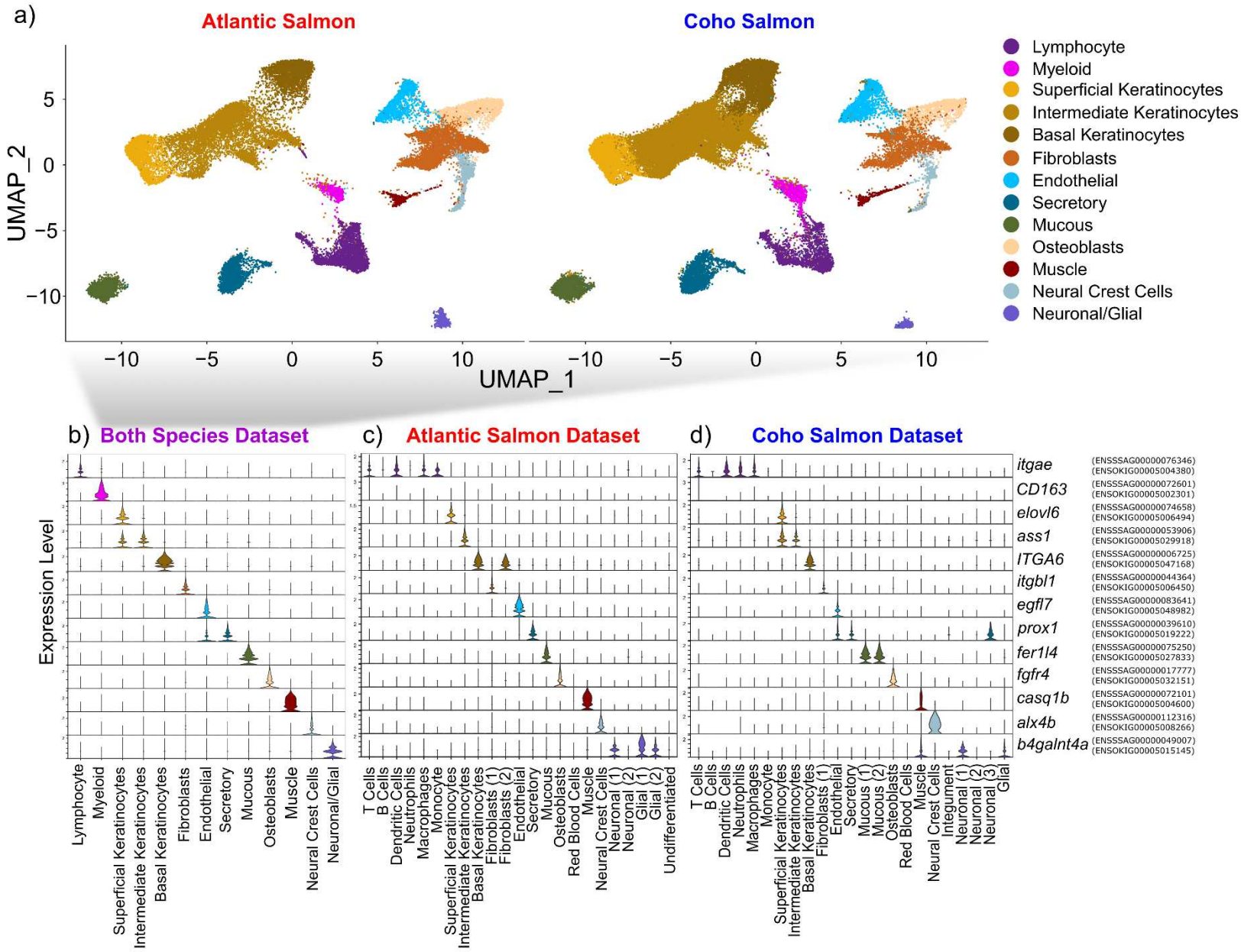

Fig.2 Cell clusters identified integrating both Atlantic salmon and coho salmon samples using 1:1 orthologous genes. a) UMAP of cell clusters split by species, b) violin plot of expression of a marker gene for each cluster. Violin plots visualize the expression of these same features in the species-specific datasets: c) Atlantic salmon, d) coho salmon. The Atlantic salmon and coho salmon ortholog ENSEMBL codes are noted to the right of each gene.

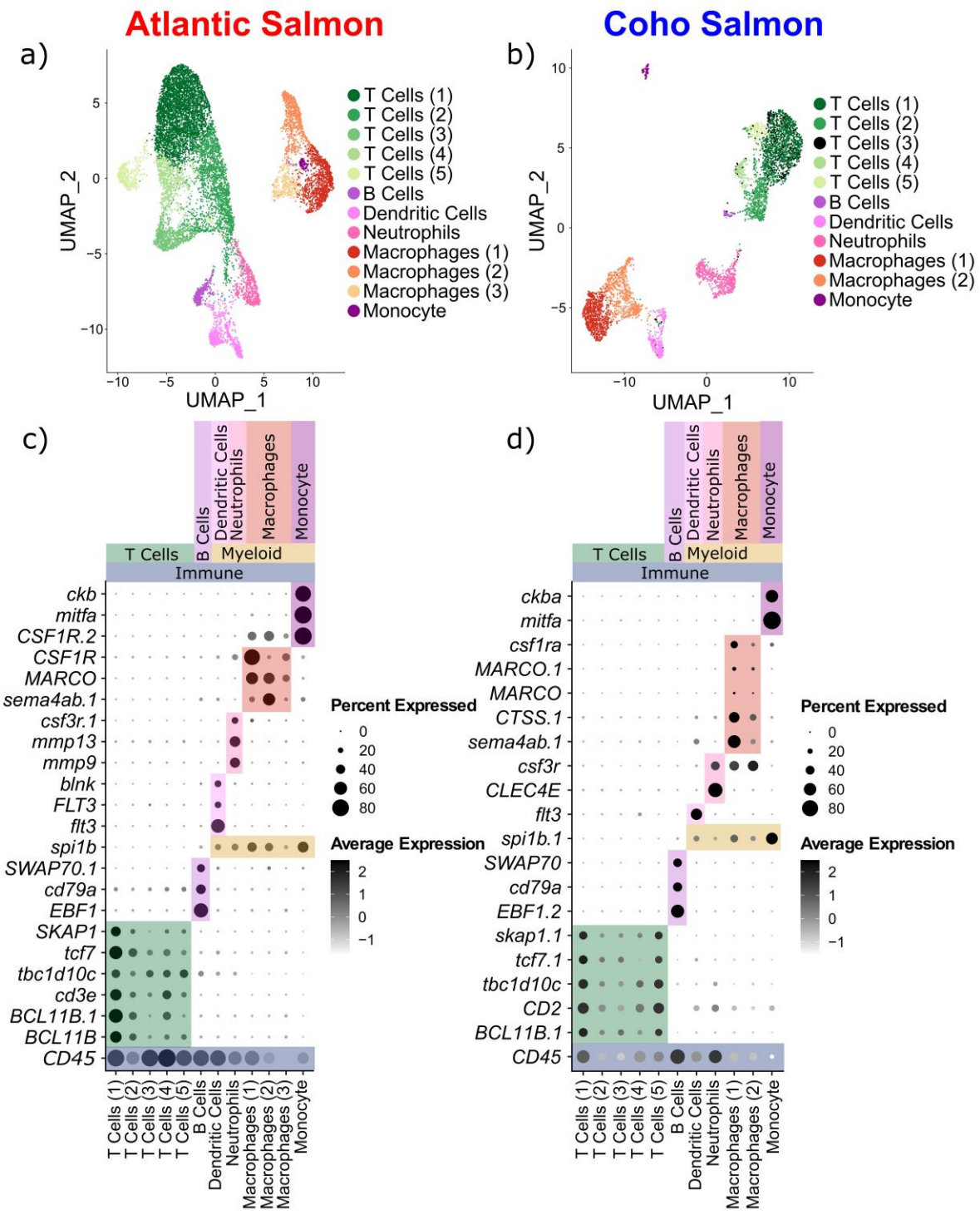

Fig.3 Sub-clustering of putative immune cells expressing CD45. UMAP visualization of immune clusters in Atlantic (a) and Coho (b) Salmon. Dot Plots of features characterizing immune cell types in Atlantic (c) and Coho (d) Salmon.

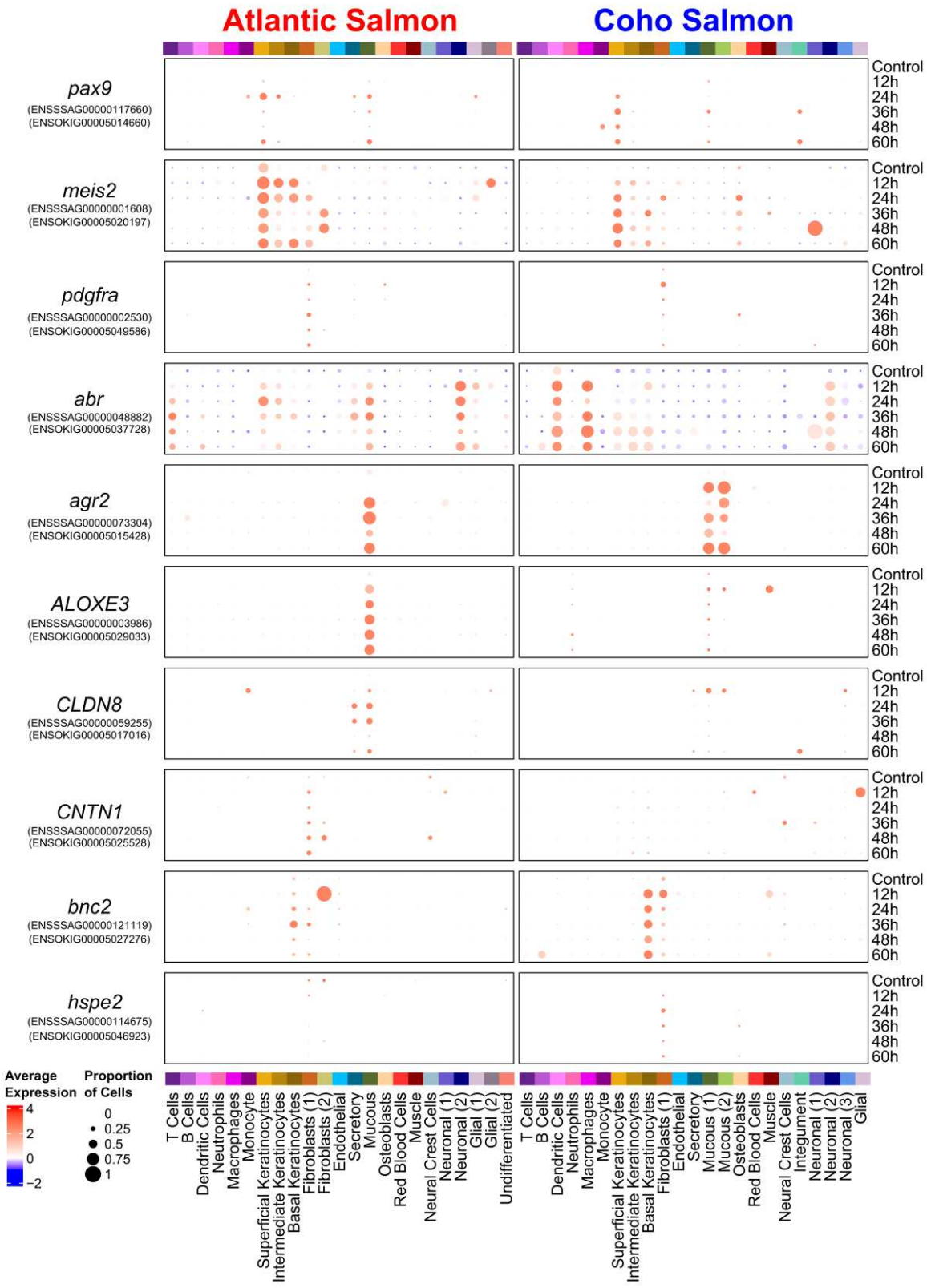

Fig.4 Dotplots of wound healing-related gene expression in Atlantic salmon and/or coho salmon in response to sea lice. All genes shown were significantly differentially expressed ($p_{adj} < 0.001$) in at least one pairwise comparison between the control and any treatment timepoint in either species.

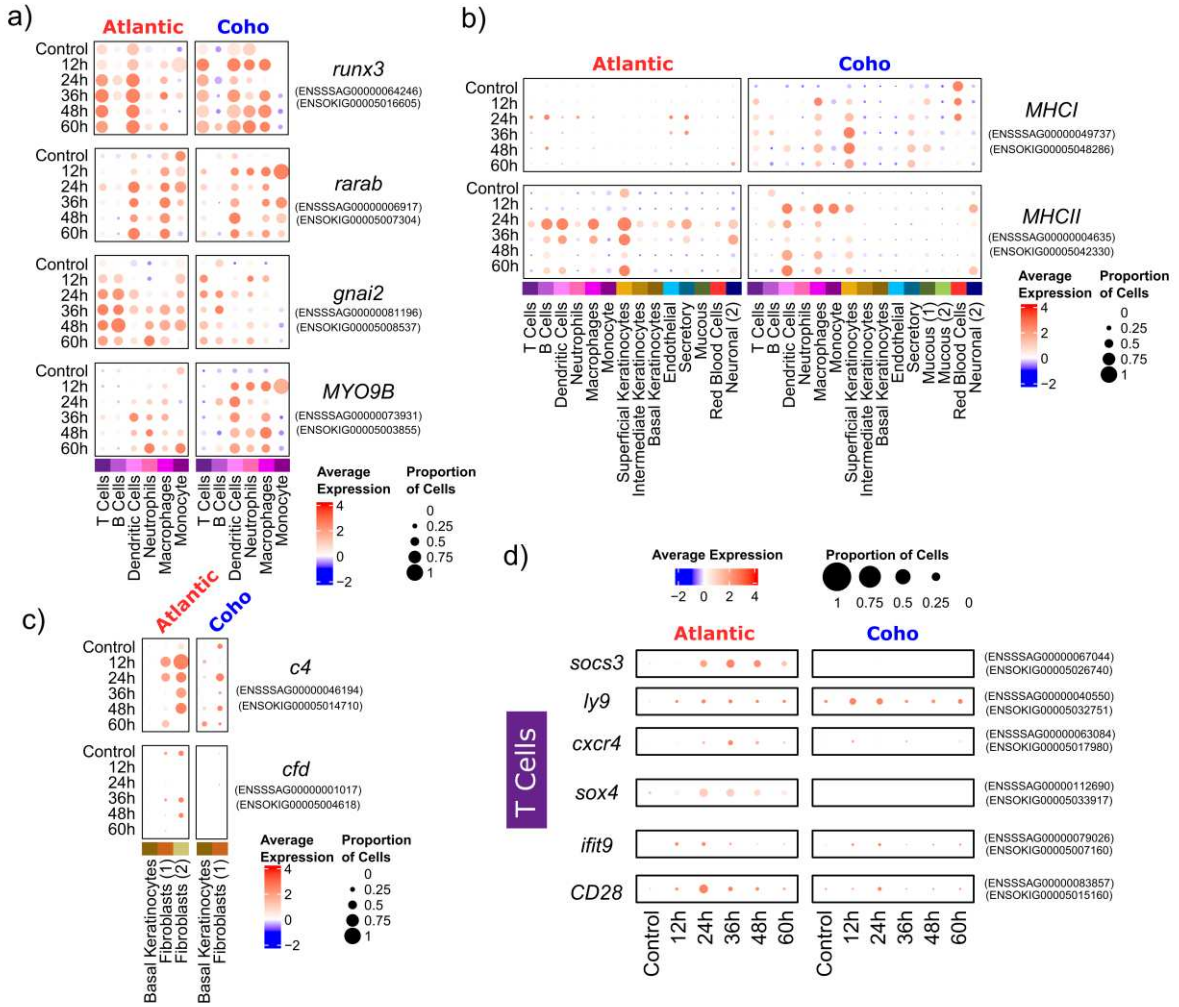

Fig.5 Dotplots of immune-related gene expression in Atlantic salmon and/or coho salmon in response to sea lice. a) immune genes upregulated in both species, b) MHC genes upregulated in both species, c) complement immune system gene expression, d) immune-related genes particularly upregulated in Atlantic salmon in response to sea lice. All genes shown were significantly differentially expressed ($p_{adj} < 0.001$) in at least one pairwise comparison between the control and any treatment timepoint in either species.

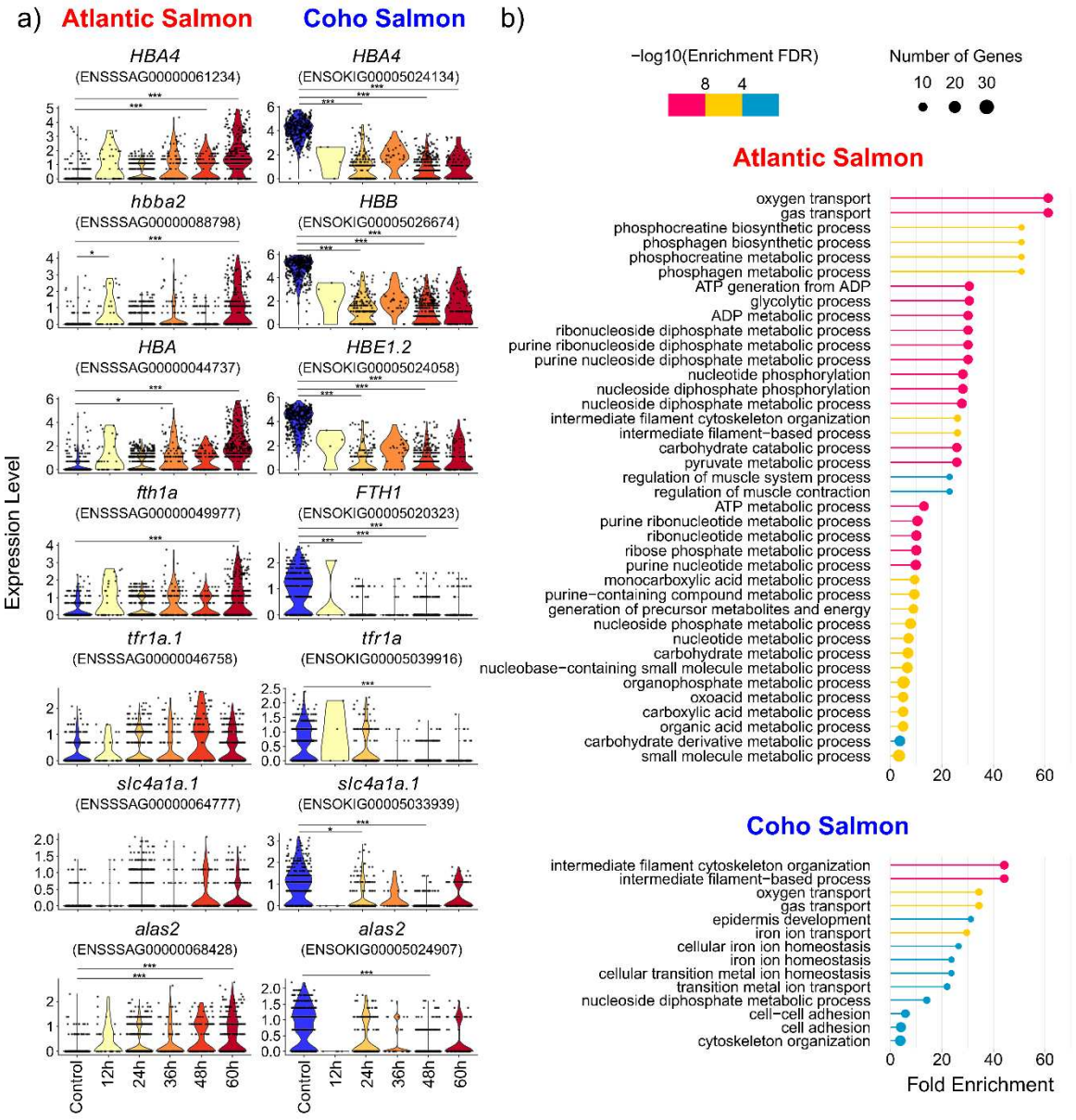

Fig.6 Red blood cell response to sea lice in Atlantic salmon and coho salmon. a) violin plots of gene expression in Atlantic salmon and coho salmon of genes significantly upregulated in coho salmon keratinocytes ($p_{adj} < 0.001$) in response to sea lice in at least one treatment timepoint relative to the control(* - $p_{adj} < 0.001$, ** - $p_{adj} < 0.0001$, *** - $p_{adj} < 0.00001$), b) significantly enriched biological GO terms (padj < 0.001) for red blood cells in response to sea lice in Atlantic salmon and coho salmon.

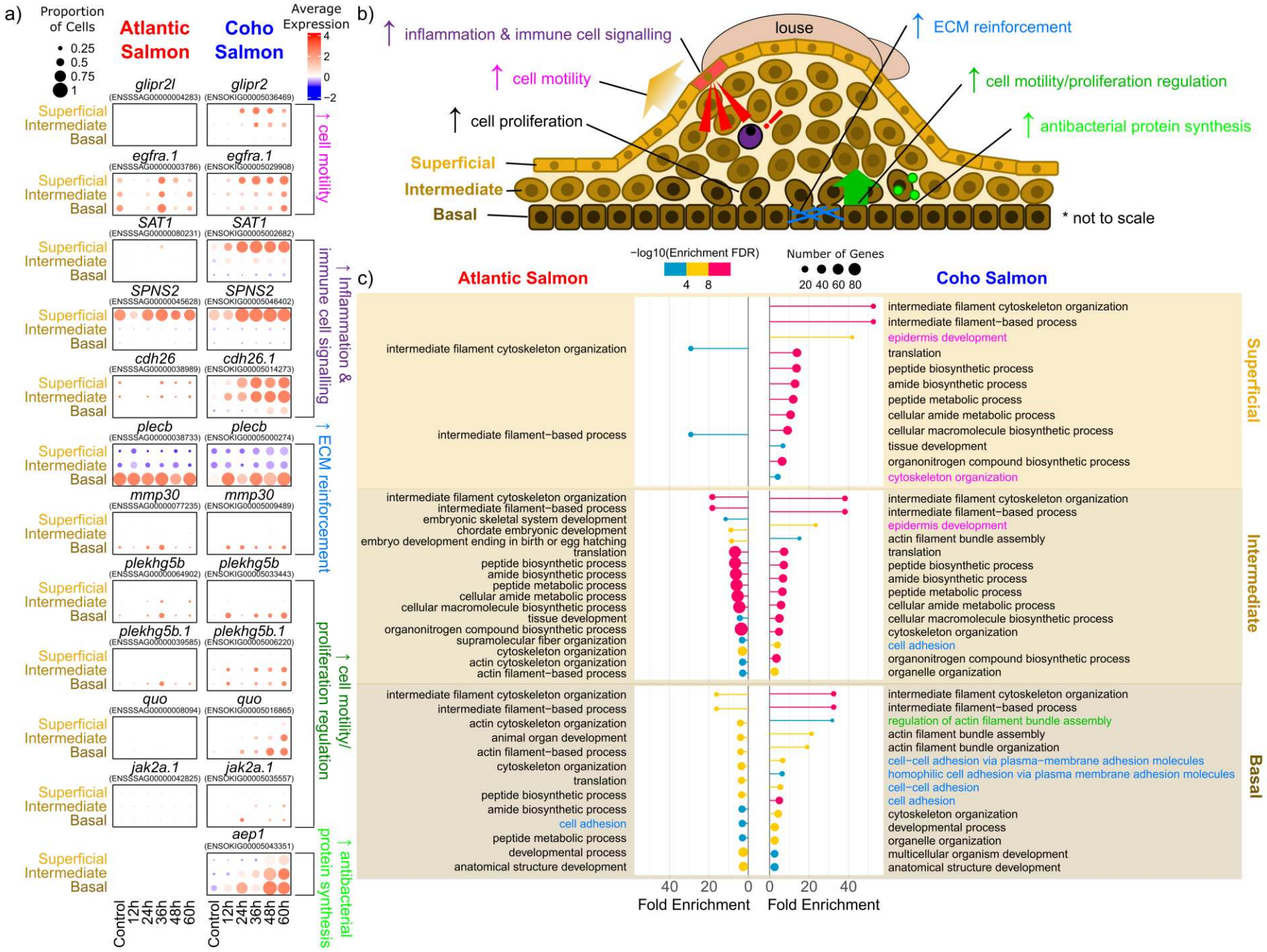
a)
Proportion of Cells
0.25
0.5
0.75
1
Average Expression
4
2
0
−2
Atlantic Salmon
Coho Salmon
glipr2l (ENSSSAG00000004283)
glipr2 (ENSOKIG00005036469)
egfra.1 (ENSSSAG00000003786)
egfra.1 (ENSOKIG00005029908)
SAT1 (ENSSSAG00000080231)
SAT1 (ENSOKIG00005002682)
SPNS2 (ENSSSAG00000045628)
SPNS2 (ENSOKIG00005046402)
cdh26 (ENSSSAG00000038989)
cdh26.1 (ENSOKIG00005014273)
plecb (ENSSSAG00000038733)
plecb (ENSOKIG00005000274)
mmp30 (ENSSSAG00000077235)
mmp30 (ENSOKIG00005009489)
plekhg5b (ENSSSAG00000064902)
plekhg5b (ENSOKIG00005033443)
plekhg5b.1 (ENSSSAG00000039585)
plekhg5b.1 (ENSOKIG00005006220)
quo (ENSSSAG00000008094)
quo (ENSOKIG00005016865)
jak2a.1 (ENSSSAG00000042825)
jak2a.1 (ENSOKIG00005035557)
aep1 (ENSOKIG00005043351)
Superficial
Intermediate
Basal
↑ cell motility
↑ Inflammation & immune cell signalling
↑ ECM reinforcement
↑ cell motility/ proliferation regulation
↑ antibacterial protein synthesis
Control
12h
24h
36h
48h
60h
b)
↑ inflammation & immune cell signalling
↑ cell motility
↑ cell proliferation
louse
↑ ECM reinforcement
↑ cell motility/proliferation regulation
↑ antibacterial protein synthesis
Superficial
Intermediate
Basal
* not to scale
c)
−log10(Enrichment FDR)
4 8
Number of Genes
20 40 60 80
Atlantic Salmon
Coho Salmon
intermediate filament cytoskeleton organization
intermediate filament−based process
embryonic skeletal system development
chordate embryonic development
embryo development ending in birth or egg hatching
translation
peptide biosynthetic process
amide biosynthetic process
peptide metabolic process
cellular amide metabolic process
cellular macromolecule biosynthetic process
tissue development
organonitrogen compound biosynthetic process
supramolecular fiber organization
cytoskeleton organization
actin cytoskeleton organization
actin filament−based process
epidermis development
actin filament bundle assembly
cell adhesion
regulation of actin filament bundle assembly
animal organ development
cell−cell adhesion via plasma−membrane adhesion molecules
homophilic cell adhesion via plasma membrane adhesion molecules
cell−cell adhesion
developmental process
organelle organization
multicellular organism development
anatomical structure development
Superficial
Intermediate
Basal
40 20 0
0 20 40
Fold Enrichment
Fold Enrichment

Fig.7 Keratinocyte response to sea lice underlies coho salmon resistance to sea lice. a) dotplots of gene expression in Atlantic salmon and coho salmon of genes significantly upregulated in coho salmon keratinocytes ($p_{adj} < 0.001$) in response to sea lice in at least one treatment timepoint relative to the control, b) proposed unique contributions of superficial, intermediate, and basal keratinocytes to epithelial hyperplasia immune response to sea lice in coho salmon, c) significantly enriched biological GO terms (padj < 0.001) for superficial, intermediate, and basal keratinocytes in response to sea lice in Atlantic salmon and coho salmon. Differentially expressed genes in a) and GO terms in c) are colour-coded by the biological processes depicted in b) that they are potentially associated with.

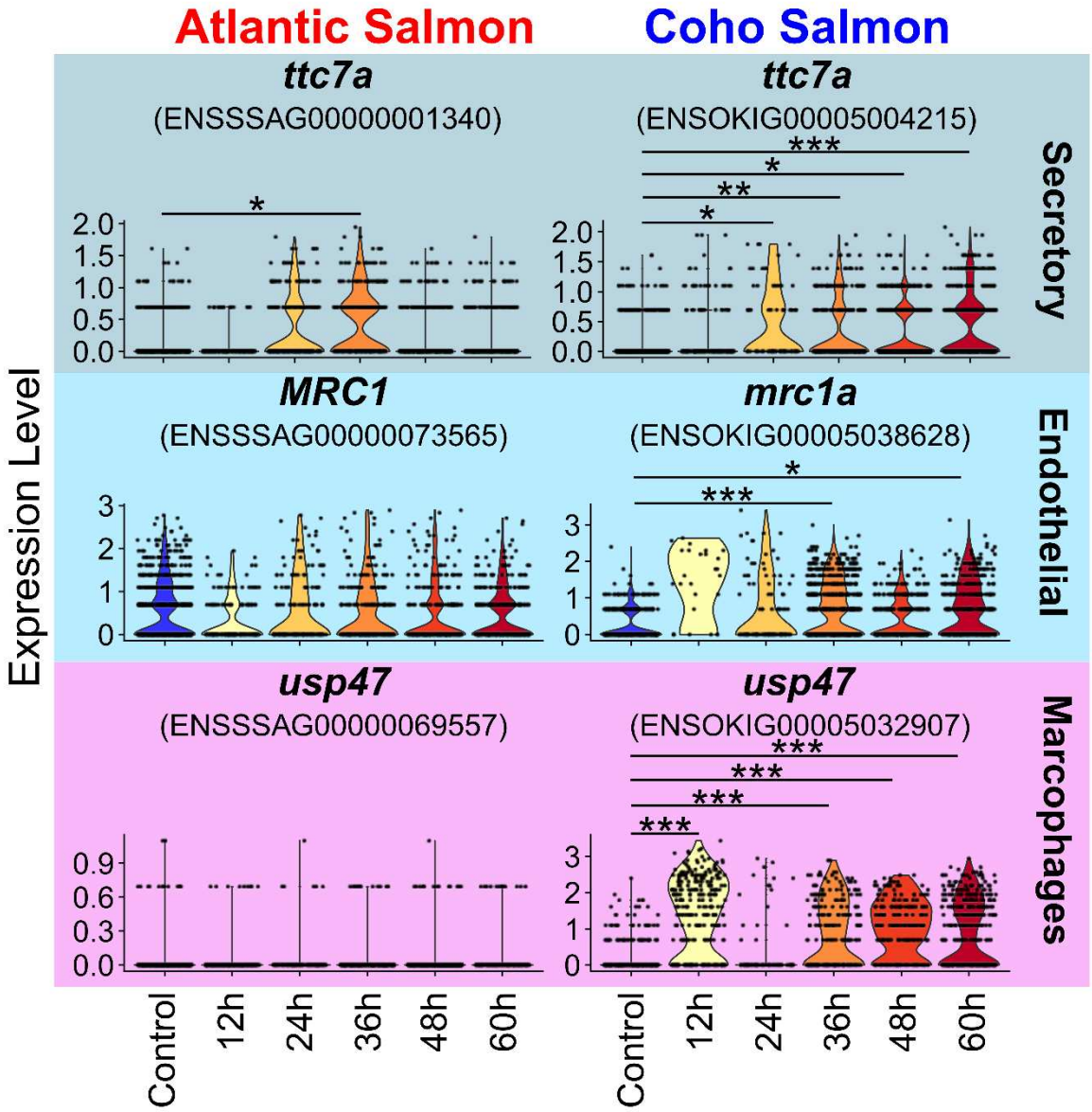

Fig.8 Violin plots of gene expression in Atlantic salmon and coho salmon in response to sea lice that are potentially regulating coho salmon's epithelial hyperplasia response to sea lice. The cell type for which the expression of each gene is shown is noted to the right of each plot. (* - $p_{adj} < 0.001$, ** - $p_{adj} < 0.0001$, *** - $p_{adj} < 0.00001$.)